Research Report 2017-08
Civil & Natural Resources Engineering

UNIVERSITY OF CANTERBURY
Te Whare Wānanga o Waitaha
CHRISTCHURCH NEW ZEALAND

LIQUEFACTION EFFECTS AND ASSOCIATED DAMAGE AT THE PORT OF WELLINGTON

Brendon, B.
Bray, J.D.
Chiaro, G.
Cubrinovski, M.J.
De la torre, C.
Olsen, M.
Wotherspoon, L.

ISSN 1172-9511

UC ENGINEERING

August 2017

LIQUEFACTION EFFECTS AND ASSOCIATED DAMAGE AT THE PORT OF WELLINGTON

Version 1.0: 22 JUNE 2017

EDITORS

Misko Cubrinovski – QuakeCoRE (NZ) Lead; University of Canterbury, Christchurch, New Zealand
Jonathan D. Bray – GEER (US) Lead; University of California, Berkeley, CA, USA

CONTRIBUTING AUTHORS (alphabetical order)

Brendon A. Bradley – University of Canterbury, Christchurch, NZ
Jonathan D. Bray – University of California, Berkeley, CA, USA
Gabriele Chiaro – University of Canterbury, Christchurch, New Zealand
Misko Cubrinovski – University of Canterbury, Christchurch, New Zealand
Christopher de la Torre – University of Canterbury, Christchurch, NZ
Michael Olsen – Oregon State University, OR, USA
Liam Wotherspoon – University of Auckland, Auckland, NZ

OTHER CONTRIBUTORS (alphabetical order)

Emilia Stocks – Tonkin+Taylor, Wellington, NZ

TABLE OF CONTENTS

ACKNOWLEDGEMENTS

Special thanks for the collaboration provided by the CentrePort Ltd. especially for allowing access to our team and making special arrangements for our multiple visits. We would like to acknowledge the great support and collaboration from Emilia Stocks, Stuart Palmer, Mike Jacka, and Sjoerd van Ballegooy, from Tonkin + Taylor, who as engineers for the CentrePort provided critical input and support in various phases of these efforts. Site access assistance through Hugh Cowan of the Earthquake Commission is sincerely appreciated. Use of results from aerial survey of Thorndon Reclamation and Wharf performed by Cardno is gratefully acknowledged.

The NZ team was principally supported by EQC Capability Grant at the University of Canterbury, and MBIE support provided for the 2016 Kaikoura Earthquake Reconnaissance. The US GEER team contributors were supported by the National Science Foundation (NSF) through the Geotechnical Engineering Program under Grants CMMI-1266418 and CMMI-1724866. Any opinions, findings, and conclusions or recommendations expressed in this material are those of the authors and do not necessarily reflect the views of the NSF. For more information visit the GEER website: www.geerassociation.org.

The NZ-US QuakeCoRE-GEER team performed on-site reconnaissance on November 17, 20, 21, 22, 23 and 30, and December 1 and 2, 2016. Profs. Misko Cubrinovski, University of Canterbury, and Jonathan Bray, University of California, Berkeley, led these QuakeCoRE-GEER efforts and participated in the inspections on multiple occasions. Christopher de la Torre (UC) contributed to most of these inspections and compilation of the gathered data. Prof. Brendon Bradley (UC), Dr. Gabriele Chiaro (UC) and Dr. Liam Wotherspoon (UA) also were members of the early reconnaissance teams. All LiDAR scanning at CentrePort was performed and processed by Prof. Michael Olsen, a U.S. GEER team member from Oregon State University, with his student, Matthew O'Banion. Leica Geosystems, David Evans and Associates, and Maptek I-Site provided equipment and/or software utilized in this study. Particle-size analyses on the ejected soils were performed in the Geotechnical Laboratory of the University of Canterbury.

This is QuakeCoRE publication number 0198 and UC Research Report 2017-8. The content is identical with Chapter 5 of GEER Report Number: GEER-053 and UC Research Report 2017-7.

1. INTRODUCTION

In the M_w7.8 Kaikoura Earthquake, the port of Wellington (CentrePort Limited) experienced liquefaction of the reclamations, lateral spreading, and ground deformations that led to building and wharf damage. The liquefaction caused global settlement of the fill deposits and lateral movement (spreading) of the fills towards the sea. There was evidence of lateral spreading in the fills behind the pile-supported wharves whereas signs of lateral spreading and liquefaction-induced settlement were evident in the soils surrounding buildings on various foundations. The QuakeCoRE-GEER team performed on-site reconnaissance on November 17, 20, 21, 22, 23 and 30, and December 1 and 2, 2016.

This report summarizes key observations from the field surveys and focuses on the geotechnical aspects of the performance of reclamations, wharves and buildings at the port. The report is organized into the following chapters: background information on the CentrePort reclamations, recorded ground motions in the context of CentrePort reclamations, observations of liquefaction manifestation and consequent ground deformation, field observations from LiDAR survey, geotechnical aspects of the seismic performance of wharf structures, and geotechnical aspects of the seismic performance of building structures.

The QuakeCoRE-GEER team included the following members:

Misko Cubrinovski – QuakeCore (NZ) Lead; University of Canterbury, Christchurch, New Zealand
Jonathan D. Bray – GEER (US) Lead; University of California, Berkeley, CA, USA
Brendon A. Bradley – University of Canterbury, Christchurch, NZ
Christopher de la Torre – University of Canterbury, Christchurch, NZ
Michael Olsen – Oregon State University, OR, USA
Liam Wotherspoon – University of Auckland, Auckland, NZ
Gabriele Chiaro – University of Canterbury, Christchurch, NZ
Matthew O'Banion – Oregon State University, OR, USA
Emilia Stocks – Tonkin+Taylor, Wellington, NZ
Richard Cole – Tonkin+Taylor, Wellington, NZ

2. CENTREPORT RECLAMATIONS

2.1 Land reclamation in the Wellington Harbour

From the early stages of European settlement and the relatively rapid expansion of Wellington in the 1840s, there was a need for reclamation in the Wellington Harbour to provide flat land for development, wider public ways, tidal protection, and deeper water along the coastline. The first notable reclamation work was along the water edge in 1847. Early reclamation works were of relatively small scale (Anderson, 1984).

Reclamation works in the Wellington Harbour were carried out in essentially three major stages: (1) early reclamations in the period 1852 – 1879; (2) early 20th century reclamations in the period 1901 – 1932; and (3) final reclamations in the period 1965 – 1975. According to Anderson (1984), until the 1960s the reclamation growth in the inner harbour and along the waterfront was a series of independent projects to serve wharves, railways, buildings, industry, and commerce rather than land formations with an overall concept. The Container Terminal of the CentrePort was established in the final stage of reclamations from 1967 to 1975.

The historical development of land reclamation in the Wellington Harbour in the vicinity of CentrePort is illustrated in Figure 2.1. In this figure, the original coastline in the 1850s is shown with the dashed line, and areas of different stages of reclamations are indicated. A large portion of the current CentrePort area was reclaimed in the final phase of reclamations between 1965 and 1975 when Thorndon Container Terminal and Thorndon Wharf were constructed. Some of the old structures from previous reclamation stages remained in place during subsequent reclamation works either as part of the current port facilities or as remnants of abandoned structures that were left in place during subsequent reclamations. The most important structures in this context are the Kings Wharf, Pipitea Wharf, and the mass concrete Old Seawall. The Kings Wharf was completed in 1906 and is part of the current port facilities, whereas the Pipitea Wharf, which was completed in 1930, was partially demolished during the Stage 3 reclamation works, but its piles and portions of the deck were left in place to provide foundation for the S37 building and are now buried in the reclaimed land. Similarly, the Old Seawall, which is aligned in the south-west to north-east direction (see Figures 2.1 and 2.2), is still in place and is part of the current reclamation. It separates the Stage 2 and Stage 3 reclamations. These structures are important references with regard to the characteristics of the reclaimed soils, because different soils and reclamation techniques were used in different stages of the reclamation works. These differences influenced the observed land performance during the Kaikoura earthquake with the old structures causing distinctly different movements relative to the surrounding reclaimed soils. Their presence was clearly manifested on the ground surface through differential settlements between the structures and their surrounding reclaimed soils.

2.2 Characteristics of reclaimed land at CentrePort

2.2.1 Construction of CentrePort Reclamation

There are several important aspects of land reclamations with regard to their performance under earthquake loading and liquefaction resistance. The composition and characteristics of soils used for land reclamation, the method of construction, and the age of the reclamation are particularly important in terms of understanding the seismic performance of the ground and structures at CentrePort.

Two methods of reclamation were primarily used to construct the reclaimed land at CentrePort: end-dumping (tipping) of gravelly soils from truck and barge operations using soils from quarries in the Wellington region, and constructing hydraulic fill using dredged material from the original seabed in the vicinity of the reclamation works. Figure 2.2 shows that hydraulic fills were constructed along the waterfront north of the Old Seawall during the second stage of reclamations whereas the majority of the reclaimed land at CentrePort was constructed by the end-tipping method. Importantly, a relatively small volume (i.e., about 250,000 m^3) of the Thorndon Reclamation might have been constructed using dredged material from the harbour entrance (Hutchison, 1973; Tonkin+Taylor, 2012).

As summarized in Figure 2.2, reclaimed land that is south of the Old Seawall is generally composed of gravelly soils with an age of approximately 40 years, with a possible exception for a relatively small volume of dredged material mentioned previously. The age of similar end-tipped gravelly reclamations north of the Old Seawall is about 100 years. The hydraulic fills, which are located north of the Old Seawall, are about 80 years old, and are predominantly composed of sand and silt dredged from the original seabed. The ages of each reclamation stage are listed in Table 2.1.

Table 2.1 Age of Reclaimed Deposits

Reclamation	Age (Years)
Stage 2 end-tipped gravelly reclamations north of the Old Seawall	100
Stage 2 hydraulic fills of dredged marine deposits	80
Stage 3 end-tipped gravelly reclamations south of the Old Seawall	40

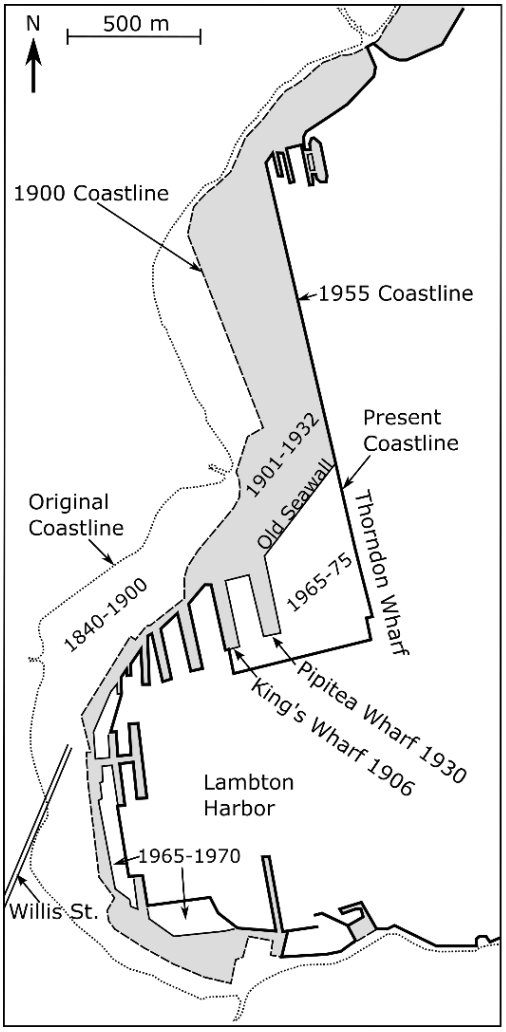

Figure 2.1: Historical development of land reclamation in Wellington Harbour (reproduced based on maps from Anderson, 1984).

Details of reclamation works performed during various development stages are relatively sparse. The characteristics of the materials used for the Thorndon Reclamation are summarized as follows (Tonkin+Taylor, 2012):

- The reclamation was constructed using "common fill." By specification, the "common fill" was gravelly soil with sand, some cobbles, and some fines; the maximum dimension of the cobbles was 150 mm (with particles larger than boulders randomly permitted); soils passing the 0.036 mm sieve should be either non-plastic or have a Plasticity Index (PI) value not greater than 5.
- A rockfill "filter" layer and overlying rockfill armour layer were placed along the edges of the slopes of the "common fill" to provide coastal protection. The rock material used for the filter was specified as a uniform material graded between 25 mm and 125 mm in diameter with up to 5% undersize material and up to 10% oversize material (up to a maximum of 300 mm in diameter). The rockfill armour was constructed of "C-grade rock" (evenly graded rock between 22 kg and 90 kg) and "A-grade rock" (graded between 90 kg and 700 kg, with at least 60% of the supplied rock

being over 450 kg). The "A-grade rock" was placed into position by a crane (i.e., it was not dropped).

The construction involved the following key stages and features:

- Prior to deposition of the "common fill" material, the seabed was dredged to remove the soft sediments.
- Approximately 2,900,000 m^3 of "common fill" from the quarries were dumped by end-tipping to construct the Thorndon Reclamation. An additional 250,000 m^3 of dredged material were also used in this reclamation.
- Fill was not compacted below the water level, because of the nature of the material used and to speed construction.
- Once the reclaimed ground reached 0.9 m above the water table, the soils were compacted to support the pavement. Static rollers (without vibration) were used to compact the fills in layers less than 0.23 m thick above the water table (WT). This created a compacted crust about 1.5 m to 2.0 m thick below the pavement.
- The reclamation was then covered by asphalt pavement overlying a base course. The thickness of the pavement varies across the reclamation area and is predominantly 0.2 m to 0.3 m thick, whereas the base course is about 0.5 m thick.
- To place the protective armour rock, small (i.e., about 6 meters wide), rock mounds were built near the toe of the "common fill" reclamation to laterally restrain the rock as it was placed over the sloped face of the reclamation fill.

2.2.2 Characteristic Layers at CentrePort

The characteristic soil profile at the Thorndon Reclamation consists of the following layers:

- Compacted earth fill and pavement layer, which is typically about 2.0 to 3.0 m thick. This layer was above the water table during construction.
- Un-compacted reclamation fill (below the WT during construction), which varies in thickness between 10 m and 18 m.
- Marine deposits of interbedded sand/clay/silty clay, or soft to very stiff clay, which are relatively thin layers with a total thickness of about 1 m to 2.5 m.
- Wellington Alluvium, which is an approximately 200-m thick layer composed of interbedded dense gravel and stiff to very stiff silt.
- Greywacke sandstone/siltstone bedrock, which is estimated to be at a depth of about 200 m to 250 m.

The thickness of the reclaimed deposit is variable depending on the horizontal distance from the original coastline (or depth to the original seabed). It is approximately 10 m to 15 m at the location of the buried mass concrete seawall (see Figures 2.1 and 2.2) and increases to approximately 18 m to 20 m at the south-most end of the Thorndon Reclamation. Underlying the reclamation fill is a relatively thin marine deposit, underlain by Wellington Alluvium.

The Wellington Alluvium is generally dense to very dense gravel with sand and silt but also consists of stiff to hard silt with sand and gravel (Tonkin+Taylor, 2012 and 2014).

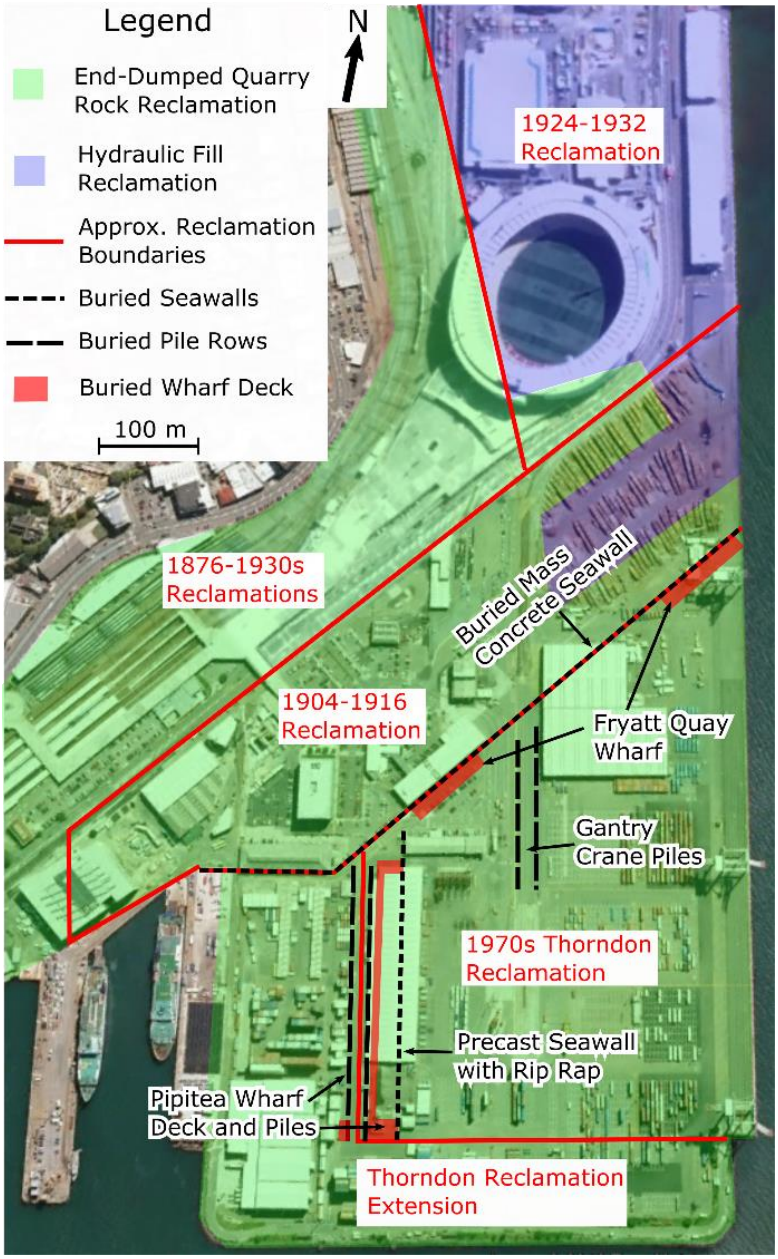

Figure 2.2: Approximate boundaries of various land reclamations at CentrePort Wellington with reference to existing and old structures and different methods of reclamation construction. (Hutchinson, 1973; Tonkin & Taylor, 2012; Semmens et al., 2010; Wellington Harbour Board, 1936. Base image from Google Earth™)

Characteristic cross sections that illustrate the key soil layers and their thicknesses are shown in Figure 2.3. The locations of these cross-sections and borings used to develop them are shown in the site plan in Figure 2.4. Mean high water (MHW) is approximately 3 meters below the existing pavement surface.

Penetration resistances are provided in the soil exploratory borings conducted at CentrePort as Standard Penetration Test (SPT) blow count data (Tonkin+Taylor; 1998, 2000, 2006, and

2012). However, the SPT procedures employed during the previous site investigations are not always described sufficiently to ascertain if the recorded N values are N_{60} values (i.e., 60% free-fall energy, which is the standard). In fact, some of the historically acquired SPT data were obtained by non-standard SPT procedures using a solid cone instead of a split-spoon sampler. SPT N values performed in the un-compacted gravelly fill range from approximately 5 to 15 blows/300 mm. In the compacted fill layer above MHW, N-values are generally in the range between 13 and 50+ blows/300 mm (Tonkin+Taylor, 2012 and 2014). SPT N values of the soil layers from some of the available borings are indicated in the simplified soil profile cross-sections shown in Figure 2.3.

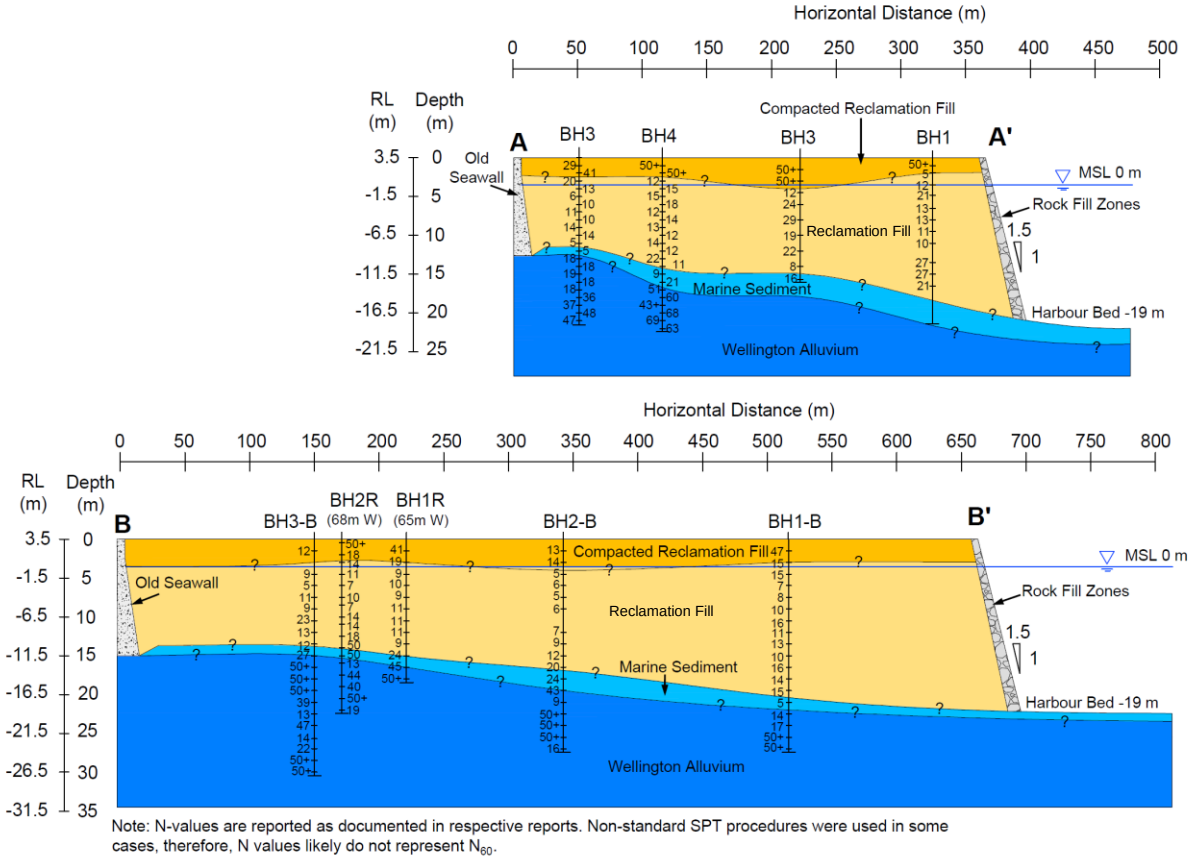

Figure 2.3: Schematic soil cross sections illustrating key layers and their thicknesses at CentrePort; note the different horizontal and vertical scales for the cross sections.

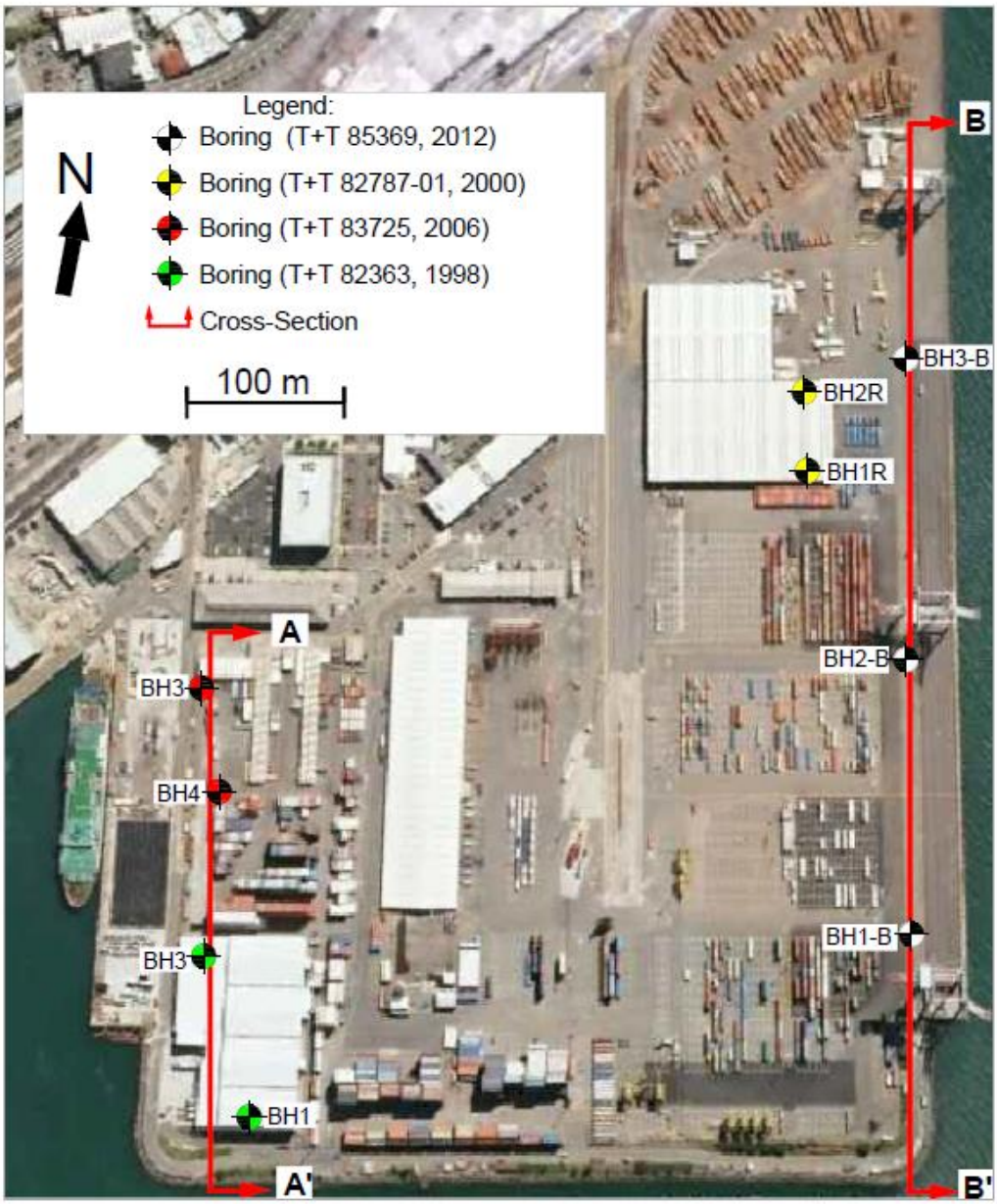

Figure 2.4: Site plan showing location of cross sections and borings used to develop the cross-sections shown in Figure 2.3; (Base image from Google Earth™).

Figure 2.5 shows grain-size distribution curves for samples (collected from subsurface explorations) of the reclaimed fill layer located approximately 5 to 40 m behind Thorndon Wharf. The fill is composed of gravelly soil including 10% to 40% sand and low fines content of less than 15%. Comparative grain-size distribution curves for samples of the marine deposits are also shown in Figure 2.5. The test data indicate the marine deposits are predominant sandy soils with fines content in the range between 15% and 35%.

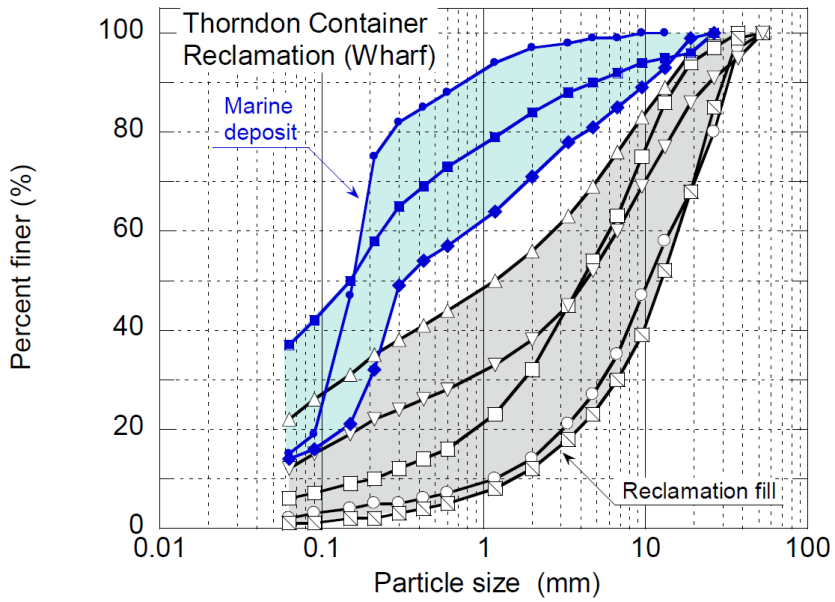

Figure 2.5: Grain-size distribution curves for borehole samples of the reclaimed fill and marine deposit.

3. LIQUEFACTION DEMAND GENERATED BY THE 2016 KAIKOURA EARTHQUAKE

3.1 Recorded ground motions

Ground motions generated by the 2016 Kaikoura earthquake were recorded by a relatively dense array of strong motion stations (SMS) in Wellington. Figure 3.1 shows the locations of eight strong motion stations (SMS) that recorded the event near CentrePort Wellington. No records were obtained directly at the Thorndon Reclamation of CentrePort. A summary of important information for the recorded accelerations and characteristics of the sites is given in Table 3.1 which includes: geometric mean horizontal peak ground acceleration (HPGA) recorded at the SMS during the 2016 Kaikoura earthquake, cyclic stress ratios at the water table (CSR_{wt}), site class per NZS1170.5, and site period estimates based on horizontal-to-vertical spectral ratios from all strong motions in GeoNet database with PGA less than 0.15 g. Note that POTS is a rock site, located about 1.0 km north-west from CentrePort. CPLB and TFSS are closest to the CentrePort; they are located about 200 m to 800 m west and northwest of the final stage reclamations at the port.

Figures 3.2 through 3.9 show ground surface acceleration-time traces and their respective 5%-damped pseudo acceleration response spectra in three orthogonal directions at stations TFSS, WEMS, CPLB, and POTS. The recorded PGAs at soil sites are generally between 0.15 g and 0.25 g (Table 3.1), and acceleration-time traces show a relatively large number of strong amplitude cycles (i.e., indicative of long significant duration) which is consistent with the $M_W = 7.8$ of the event. These ground motion characteristics on their own indicate that this area of the Wellington Harbour and CentrePort itself were subjected to significant seismic demand (earthquake loading).

The QuakeCoRE-GEER team inspected each of the SMS sites mentioned previously. There was no evidence of liquefaction manifestation in the form of sediment ejecta at the ground surface at any of these SMS sites. CPLB is at the B building, the perimeter of which was documented in brief walk-through inspections. A small settlement of the surrounding soil relative to the B building was observed at some locations. At other locations, the settlement of the ground relative to the building was negligible to minor. There was no evidence of significant ground deformation at any of the other SMS sites.

As mentioned earlier, POTS is located on rock and therefore, is valuable as a reference site for investigation of basin effects and local soil response (site effects) on the recorded motions in the Kaikoura event. It could also be beneficial for performing seismic site response analyses of various sites (including SMS sites) at which nonlinearity and liquefaction may have significantly influenced the response. Figure 3.10 shows envelopes of 5%-damped elastic pseudo-acceleration response spectra, for the eight SMS sites considered, grouped in terms of site characteristics as: rock (POTS), natural soil deposit (VUWS, WEMS), and reclaimed soil sites (PIPS, TFSS, CPLB, FKPS, TEPS). The plots for the reclaimed soil sites have been shown with and without FKPS and TEPS spectra, because these two sites are affected by the Te Aro Basin as opposed to the Thorndon Basin effects at CentrePort and

nearby SMS sites. The spectra reflect the combined effects of several factors including depth to bedrock, soil response, and basin geometry in conjunction with the excitation characteristics (e.g., source and path effects). The complex potential influence of various factors should be considered when interpreting the recorded ground motions. The comparative plots show strong amplification of amplitudes at both natural and reclaimed sites as compared to the rock accelerations across all periods up to 4 seconds. The amplification is particularly pronounced in the range between T = 1.0 s and 2.0 s, and for this and greater periods is more pronounced at the reclaimed sites located along or closer to the waterfront. In Figure 3.10(a), the enveloped geometric mean spectra are compared to the design spectrum from NZS1170.5 for Site Class D (SNZ 2004). Observed ground motions exceeded this design spectrum only at periods between approximately 1 and 2 seconds for sites on reclaimed soil, and are significantly less than the design spectrum at periods shorter than 1 seconds and longer than 2 seconds.

Table 3.1: Strong motion stations near CentrePort with geoemetric mean PGA for the 2016 Kaikoura earthquake and site characterisation metrics.

Station ID	**Kaikoura EQ Geomean HPGA (g)**	**CSR_{wt} = 0.65 PGA/g**	**NZS1170 .5 Site Class**	**Site Period Estimate (sec)**	**Site (soil) type**
POTS	0.074	-	B	-	Rock
TFSS	0.177	0.11	D	1.3	Natural soil deposit
WEMS	0.146	0.09	D	0.80	Natural soil deposit
CPLB	0.235	0.15	D	1.2	Reclaimed soil
VUWS	0.198	0.13	D	0.75	Reclaimed soil
TEPS	0.126	0.08	D	1.0	Reclaimed soil
FKPS	0.159	0.10	D	1.0	Reclaimed soil
PIPS	0.240	0.16	Unknown	> 2	Reclaimed soil

Figure 3.1: Aerial view of Wellington highlighting CentrePort. The location of strong motion stations near CentrePort Wellington that recorded the Kaikoura earthquake are also shown (Base image from Google EarthTM).

TFSS – Wellington Thorndon Fire Station

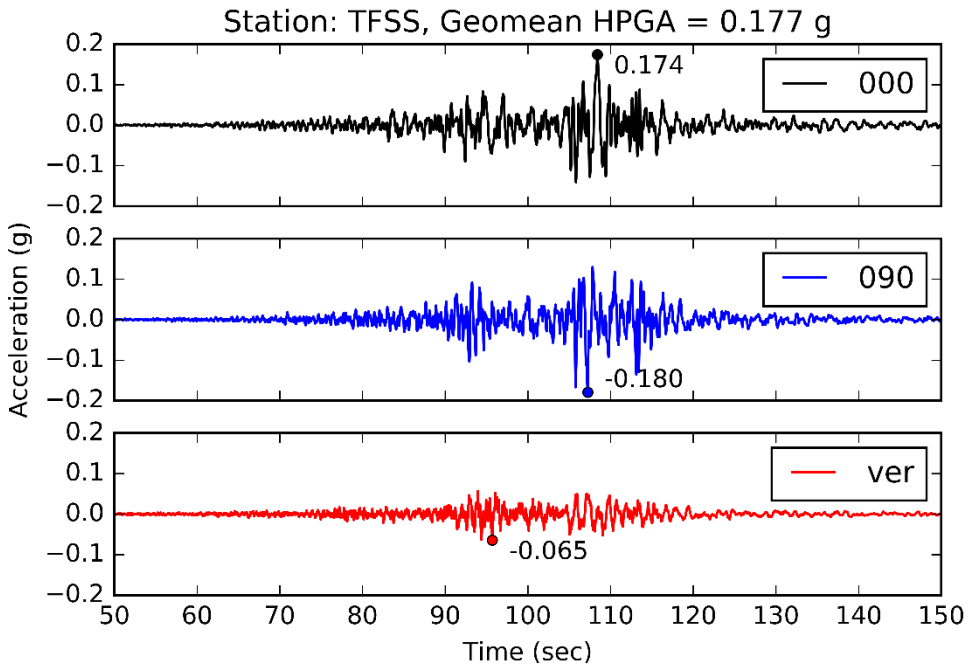

Figure 3.2: Acceleration traces from station TFSS.

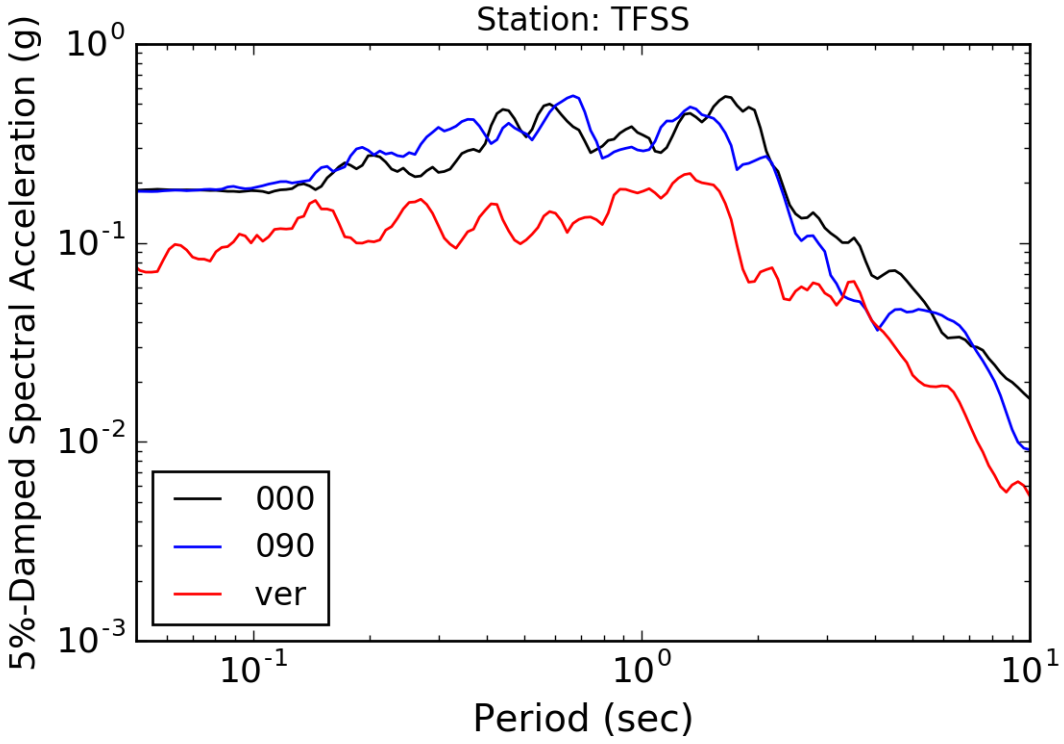

Figure 3.3: Acceleration response spectra (5% damped) from TFSS station recording.

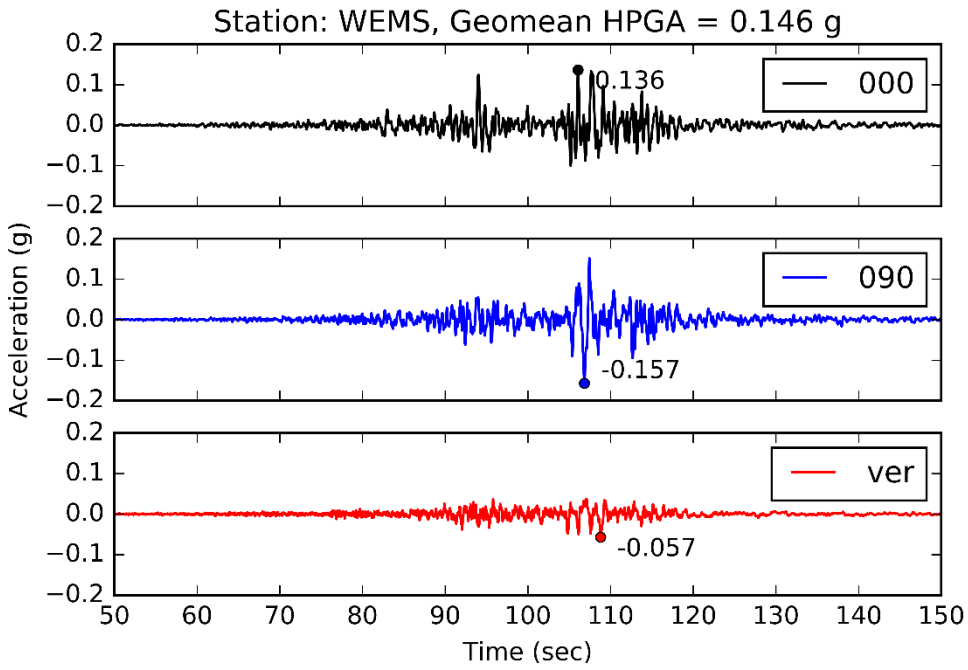

Figure 3.4: Acceleration traces from station WEMS.

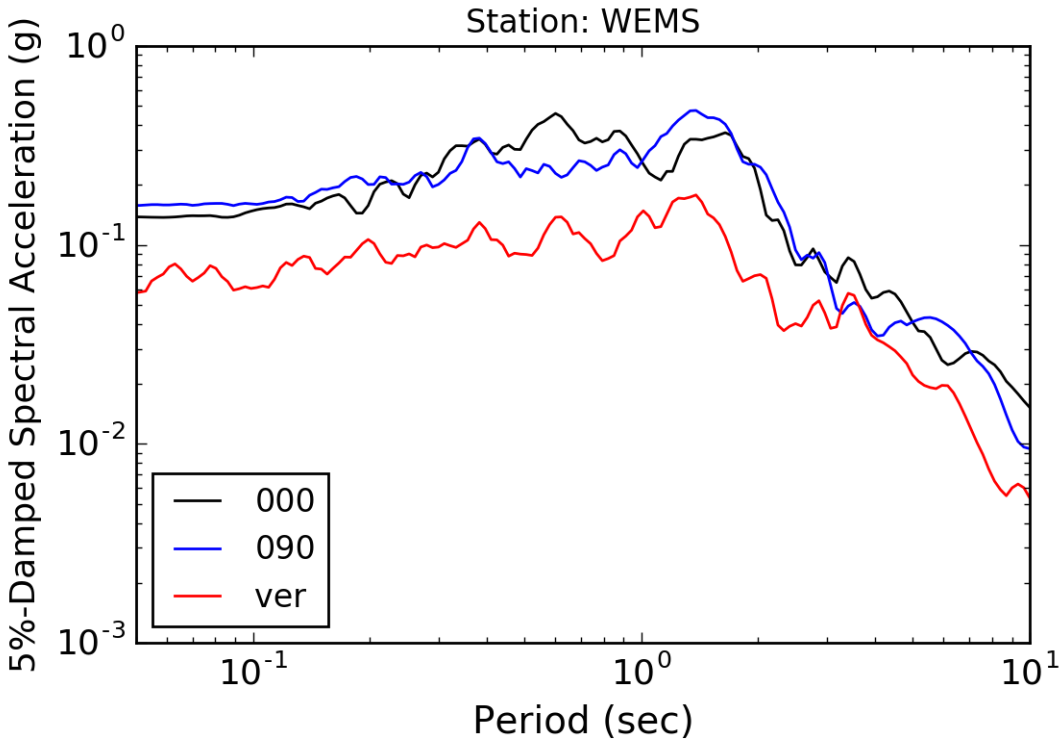

Figure 3.5: Acceleration response spectra (5% damped) from WEMS station recording.

CPLB – Wellington CentrePort BNZ Building

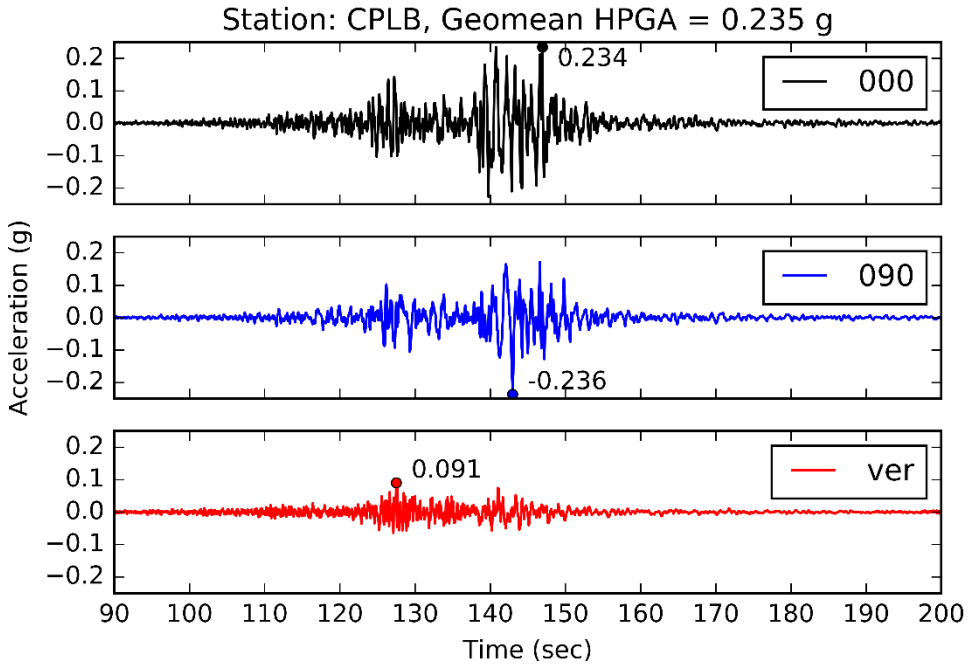

Figure 3.6: Acceleration traces from station CPLB.

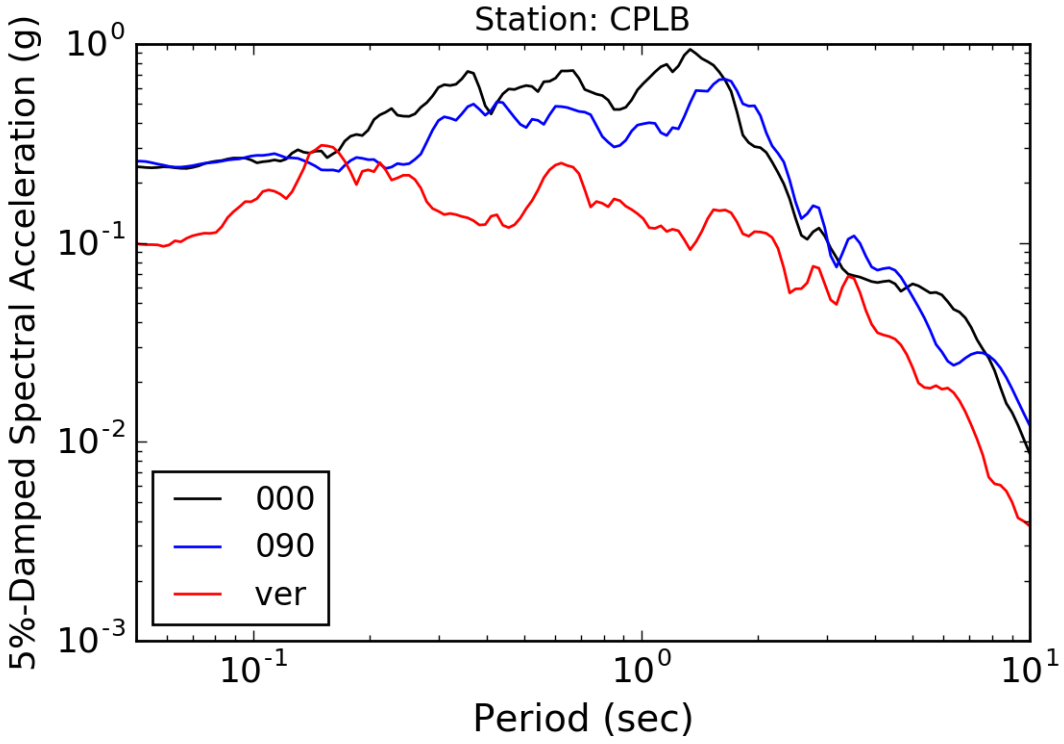

Figure 3.7: Acceleration response spectra (5% damped) from CPLB station recording.

POTS – Wellington Pottery Association

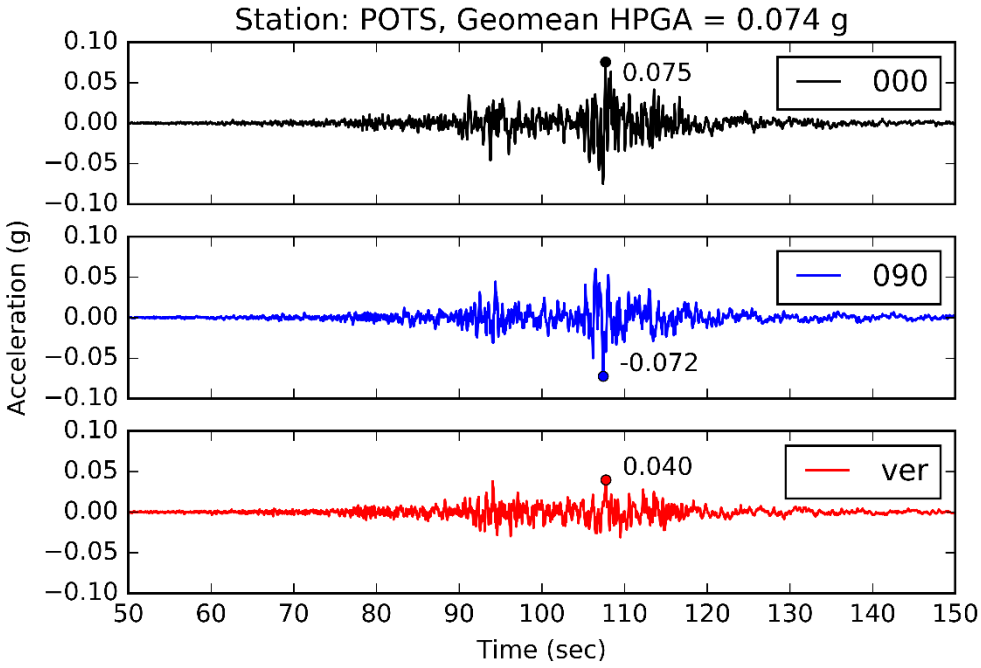

Figure 3.8: Acceleration traces from station POTS.

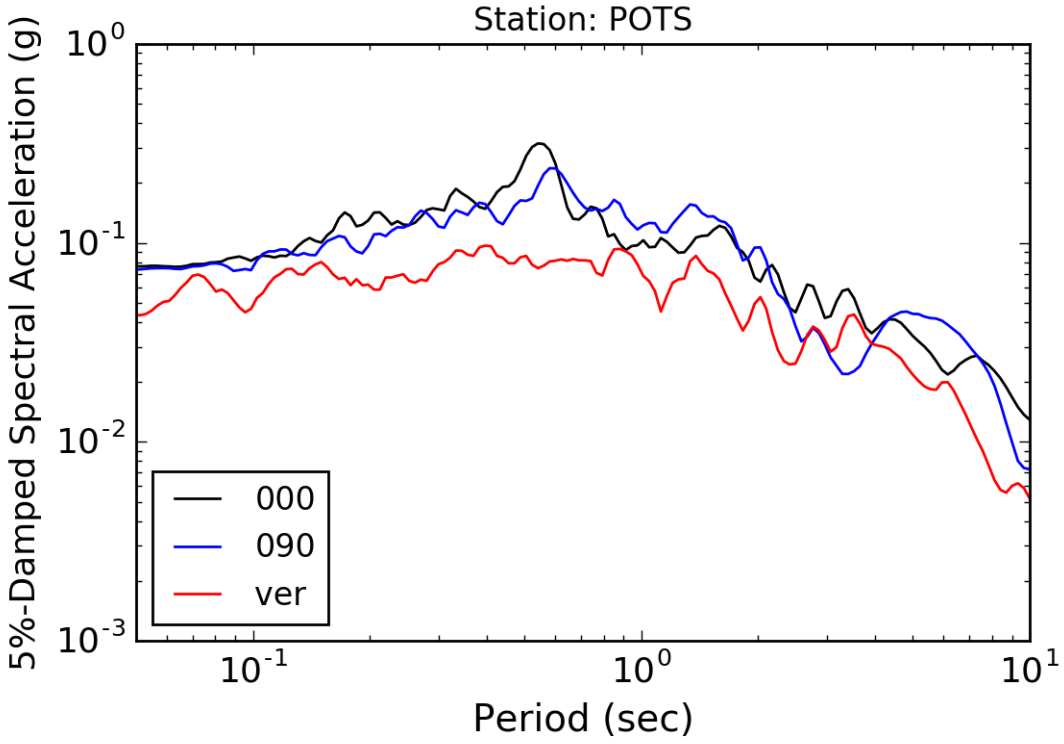

Figure 3.9: Acceleration response spectra (5% damped) from POTS station recording.

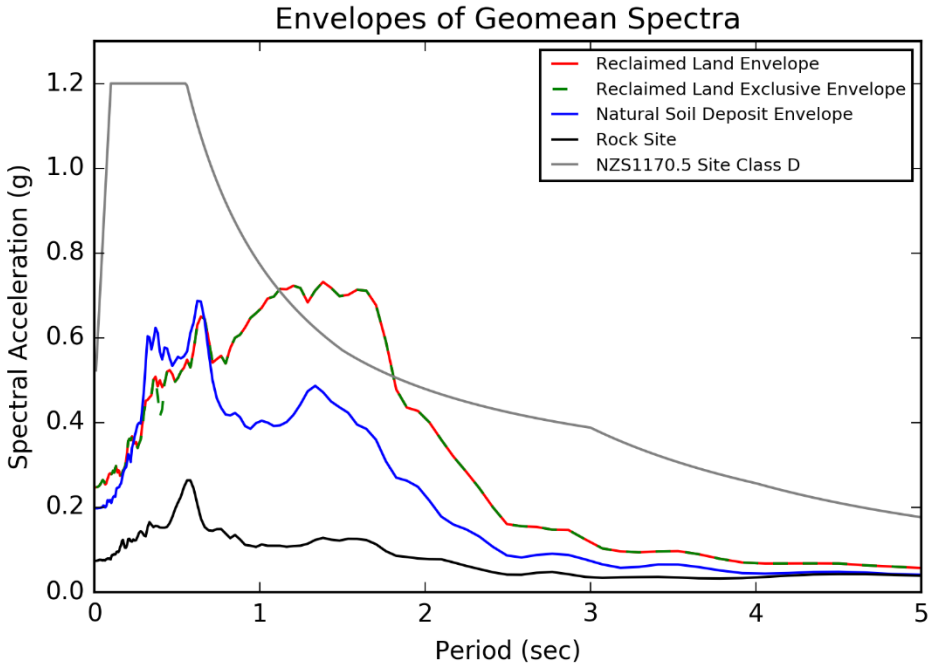

(a)

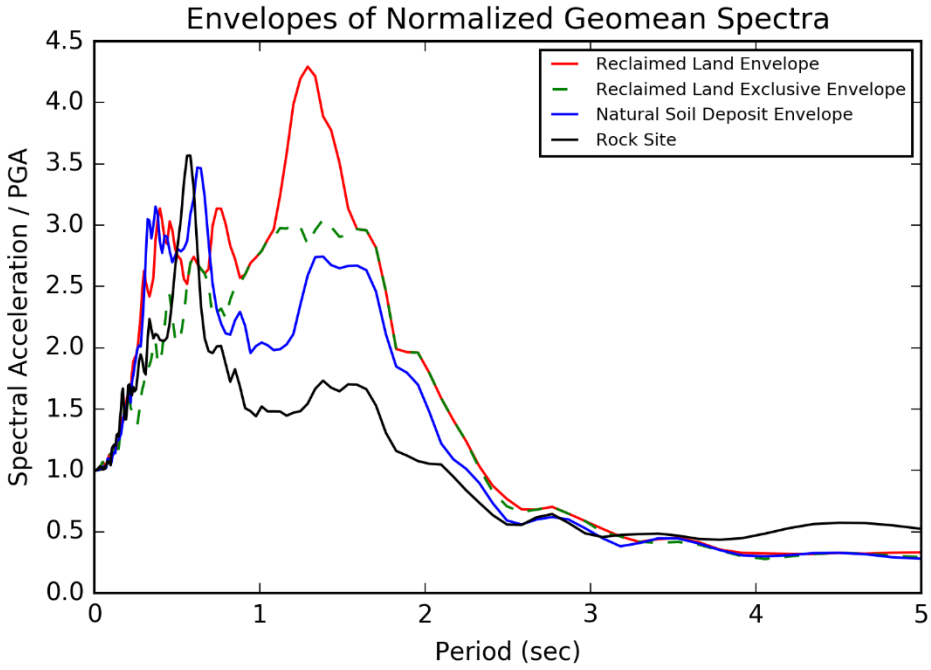

(b)

Figure 3.10: Acceleration response spectra (5% damped) for rock, natural deposits, and reclaimed soils sites: (a) envelopes of geometric mean horizontal acceleration response spectra (NZS1170.5 design spectrum is also shown for reference); (b) envelopes of normalized geometric mean spectra.

3.2 Seismic demand for liquefaction assessment

In the widely used simplified liquefaction triggering procedures (e.g., Boulanger and Idriss, 2014), a factor of safety against liquefaction triggering is estimated as

$$FS = \frac{CRR_{7.5,100}}{CSR} MSF \times K_\sigma \qquad (1)$$

in which $CRR_{7.5,101}$ is the Cyclic Resistance Ratio for a M_w7.5 event and an effective overburden stress of 101 kPa (atmospheric pressure) at a level ground site, MSF is the magnitude scaling factor, K_σ is overburden stress correction factor, and CSR is the Cyclic Stress Ratio, which is a proxy for the amplitude of the seismic demand. CSR is a function of the PGA at the ground surface, the ratio of the total and effective vertical stresses, the depth within the deposit, and the depth below the water table, i.e. CSR = $f[PGA, \sigma_{vo} / \sigma'_{vo}, r_d(z), z_{wt}]$. For shallow depths at the water table, the depth dependent factors are equal to unity (i.e., there are no effects of soil flexibility [r_d = 1.0], water table depth on CSR [$f(z_{wt})$ =1.0], and $\sigma_{vo} / \sigma'_{vo}$ = 1.0 at the water table). Hence, the cyclic stress ratio is effectively a function of the PGA alone. With these simplifications in mind, the cyclic stress ratio at a shallow depth of the water table (CSR_{wt}) can be approximated with Equation 2 using the geometric mean peak ground accelerations (a_{max}) recorded in the horizontal directions at the strong motion stations:

$$CSR = 0.65 \frac{a_{max}}{g} \qquad (2)$$

The estimated CSR_{wt} values for the SMS sites are summarized in Table 1. CSR_{wt} = 0.11 – 0.16 for the three SMS sites closest to the port (i.e., CPLB, TFSS, and PIPS). This demand in terms of CSR is illustrated in Figure 3.11 together with the equivalent sand liquefaction resistance ($CRR_{7.5,101}$) as a function of the SPT blow count (shown with the solid line), as defined in the semi-empirical liquefaction evaluation procedure of Boulanger and Idriss (2014). Note that the product of $MSF \times K_\sigma$ in Equation (1) is approximately 1.0 for the combination of M_w7.8 earthquake and an effective overburden stress of about σ'_{vo} = 40 to 60 kPa corresponding to a water table depth of 2 m to 3 m. Thus, the computed CSR_{wt} can be directly compared to the liquefaction resistance expressed in terms of $CRR_{7.5,101}$ shown in Figure 3.11. If one accounts for the conservatism in this deterministic relationship of $CRR_{7.5,101}$, which corresponds to a 15% liquefaction probability (Boulanger and Idriss, 2012), then the plot roughly indicates that the seismic demand was sufficient to trigger liquefaction in deposits having an equivalent clean sand SPT blow count of less than 10 to 14 blow counts. This simplified estimate of seismic demand applies to the soil at the depth of the ground water table and serves only as a rough indicator of the imposed seismic demand for assessing liquefaction triggering. The Boulanger and Idriss (2014) CRR correlation was developed based on case histories on sandy soils, and therefore its applicability to gravelly soils is affected by several factors including the conversion of the penetration resistance of gravelly soils to an equivalent clean sand blow count. Hence, the plot shown in Figure 3.11 is only an indicator of the seismic demand in relative terms (i.e., in relation to an equivalent clean sand liquefaction resistance), and further research is needed to determine directly the cyclic resistance of the reclaimed deposits.

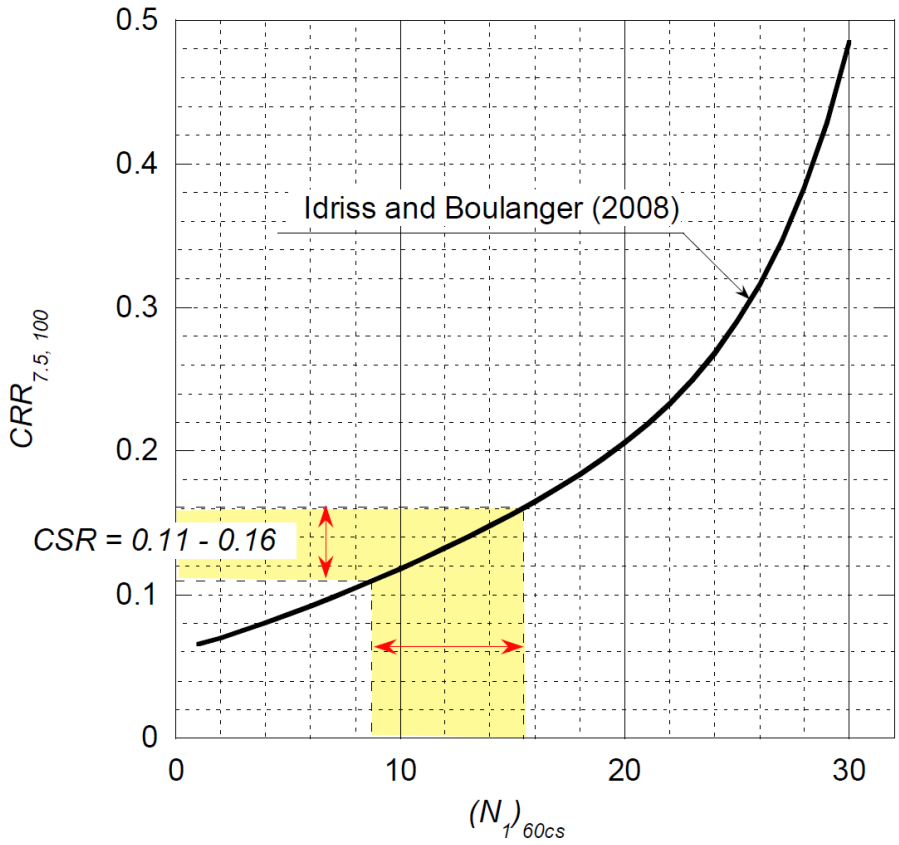

Figure 3.11: Illustration of seismic demand for assessing liquefaction triggering by the 2016 Kaikoura earthquake at depth of the water table for the three sites on reclaimed soils in the vicinity of the port (PIPS, TFSS and CPLB).

4. LIQUEFACTION-INDUCED LAND DEFORMATION

4.1 Introduction

The first QuakeCoRE-GEER team survey at CentrePort was conducted on 17 November 2016, three days after the earthquake, while most of the liquefaction evidence remained on the ground surface. These inspections covered most of the port area and focused on documenting key observations on the seismic performance of the reclamations, and wharf and building structures including measurements of vertical offsets and horizontal movements along selected transects, and collecting representative samples of the ejected materials from various locations at the port. Subsequent surveys were performed from 20 November to 1 December, which focused on obtaining additional evidence and measurements of ground movements and relative movements between the wharves or buildings and the surrounding soils. In the later part of this period, ground-based LiDAR scanning was conducted along transects of the reclamations and around and within structures of interest. The observations and measured values (approximate values obtained from measurements during the inspections) presented in this document were obtained from the above field reconnaissance activities, if not stated otherwise. Additional detailed observations have been compiled and shared when permitted by the CentrePort Limited.

4.2 Liquefaction Manifestations

Relatively widespread liquefaction was observed in both the end-dumped quarry fill and hydraulically-placed dredged fill. Liquefaction was manifested in various forms either directly as soil ejecta on the pavement surface of the port or indirectly in the form of vertical and horizontal ground movements often accompanied by ground cracks and fissures, or vertical offsets especially along the interface zones with wharves and buildings. From these general observations, one could infer a substantial global (mass) settlement across much of the reclamation, and lateral movement (spreading) of the fills towards the sea. These lateral movements and associated ground distress were generally more pronounced along the edges of the reclamation. The ground movements affected the wharves and buildings at CentrePort in various ways, as discussed in Chapters 6 and 7 of this report, respectively.

The liquefaction was most evidently manifested by ejected soils on the paved surface of the port. The areas covered by ejecta were scattered and somewhat non-uniform both in their spatial distribution and thickness of the ejected soils. The manifestations of liquefaction varied from traces of ejected soil and water to larger volumes of ejecta with thicknesses of up to 150 mm to 200 mm. The latter were typically found near cracks and fissures through which the liquefied soils reached the ground surface. In a few isolated cases, a larger amount of ejecta was observed near partially collapsed pavement and cavities, or along existing drainage conduits beneath the pavement.

The ejected soils in the area south of the Old Seawall (i.e., in the area of the end-tipped 'common fill' reclamation) consisted of gravelly soils including some cobble-sized particles. There was one notable exception in this regard, where a smaller area of the Thorndon Container Terminal was covered by uniform sand ejecta. Sand ejecta was also observed in the hydraulically-placed fill of the Log Yard, north of the Old Seawall.

The photos shown in Figures 4.1 to 4.5 illustrate some of the key liquefaction manifestation features observed in several areas of CentrePort.

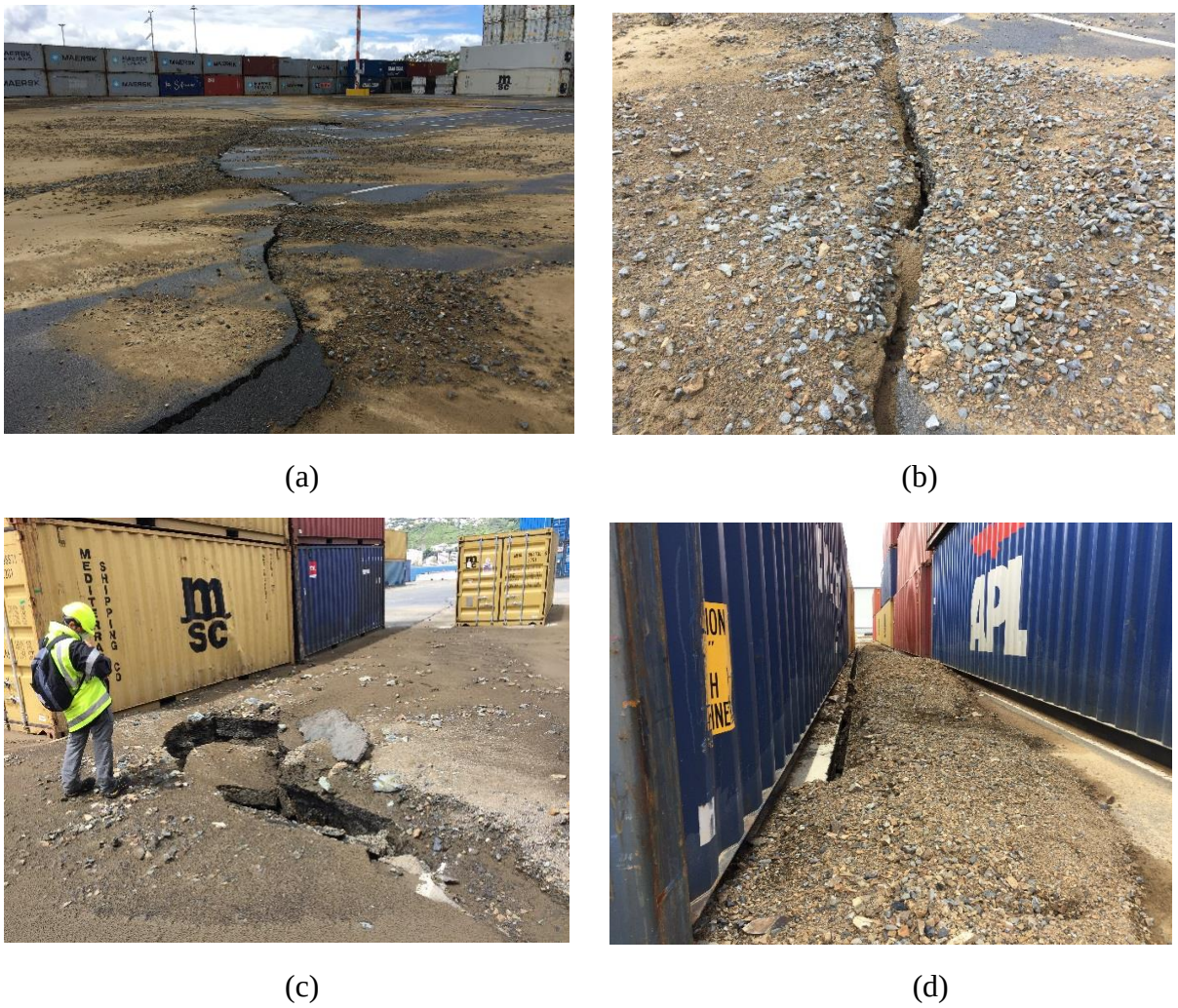

(a) (b)

(c) (d)

Figure 4.1: Gravelly ejecta at the Thorndon Container Terminal: (a) pavement cracking and ejected gravelly material (S41.280175°, E174.787308°); (b) characteristic gravel-size fractions of the ejecta with some cobbles observed in this area (S41.280206°, E174.787431°); (c) larger amount of gravelly ejecta around a cavity and collapsed pavement surface (S41.280361°, E174.789336°); (d) large volumes of ejecta observed along drainage lines (S41.278347°, E174.788069°, taken on 17NOV16).

(a) (b) (c)

(d) (e)

Figure 4.2: High gravel content quarry rock ejecta in the container storage area upland of Thorndon Container Wharf. (a) Looking south along eastern wall of Substation B (S41.277699°, E174.788277°), (b) looking south along lateral spread crack and ejecta 45 m upland of bulkhead at approximately STA 230 (S41.278286°, E174.788830°), (c) coarse gravel and cobble ejecta (S41.280225° E174.787828°), (d) containers 20 m south of Substation B (S41.278020°, E174.788213°), and (e) looking south along lateral spread crack and ejecta 12.5 m upland of bulkhead at approximately STA 150 (S41.278887°, E174.789413°, taken on 21NOV16).

Figure 4.3: Sandy liquefaction ejecta with trace gravel among area of 1970's end-dumped quarry rock reclamation (i.e., Thorndon Reclamation) at STA 145 and approximately 60 m upland of the bulkhead. The ejecta deposit was approximately 170 mm thick at this location. Samples S11 and S12 were collected here (S41.279067°, E174.788792°, taken on 17NOV2016 and 21NOV16).

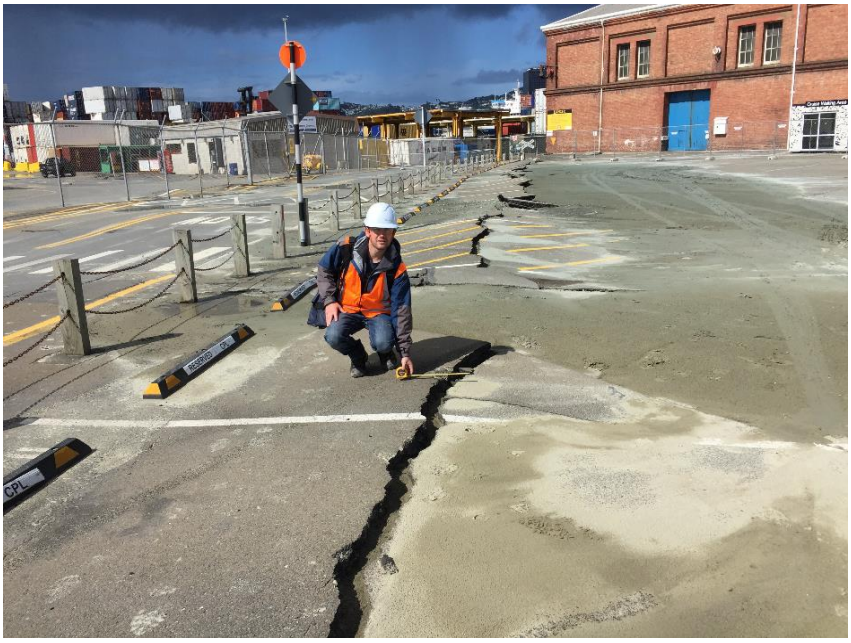

Figure 4.4: Sandy liquefaction ejecta behind buried mass concrete seawall looking southwest along seawall. On the right side of seawall: area of end-dumped quarry rock reclamation from 1904-1916 (Sample S2), left side of seawall: area of end-dumped quarry rock reclamation from 1970's Thorndon Reclamation. (S41.278454°, E174.785154°, taken on 17NOV16)

Figure 4.5: Sandy liquefaction ejecta in the log stacking area in the northeast corner of CentrePort (Sample S13). Area of hydraulic fill reclamation. (S41.274972°, E174.788347°, taken on 17 NOV16)

During the first field survey on 17 November, several ejecta samples were collected for index testing in the laboratory. Thirteen of those samples, indicated as S1 to S13 in this report, were collected from the locations shown in Figure 4.6. Sand liquefaction ejecta were observed at three different areas. These areas are: (1) in the Thorndon container stacking area at samples S11 and S12 (Figure 4.3), (2) immediately upland of the buried mass concrete seawall at sample S2 (Figure 4.4), and (3) in the log stacking area at sample S13 (Figure 4.5). Interestingly, only the log stacking area at S13 coincides with mapped area of sandy hydraulically-placed dredged fill (i.e., purple shaded area in Figure 2.2). Gravelly liquefaction ejecta were present over large portions of the Thorndon Reclamation and the Thorndon Reclamation Extension. This material is the end-dumped quarry rock referred to above as "common fill." The remaining samples were collected from this material. Several photos of this gravelly liquefaction ejecta are shown in Figures 4.1 and 4.2.

Grain size distribution curves obtained in the laboratory for the 13 ejecta samples are shown in Figures 4.7c and 4.7d where gravelly and sandy soils ejecta are shown respectively. The shaded areas in the background of these figures show the range of grain size distributions for the reclamation fill and marine deposit samples (collected from subsurface explorations) indicated in Figure 2.5. The grain-size curves of the gravel ejecta (solid lines in Figure 4.7c) are in good agreement with the grain-size distribution range of the gravelly soils of the

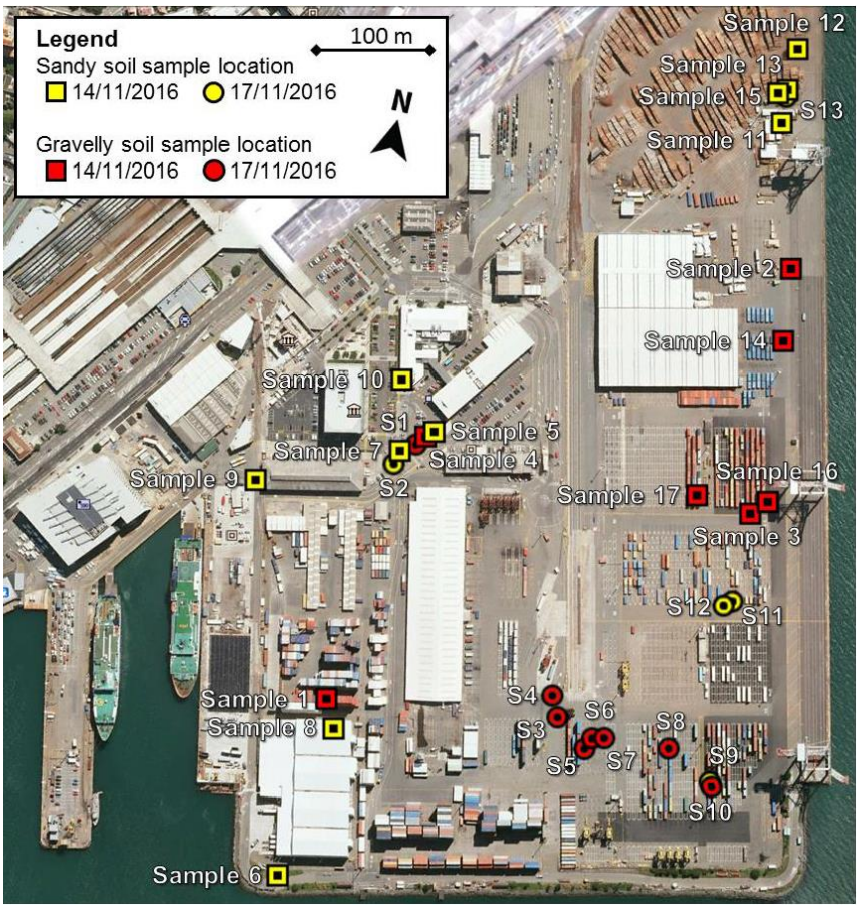

Figure 4.6: Location of liquefaction ejecta samples collected on 14 November (Sample 1 to Sample 17), and 17 November (S1 to S13). (Base image from Google Earth™)

Thorndon reclamation (shaded zone in Figure 4.7c). Similarly, the grain-size distribution curves of the sand ejecta (solid lines in Figure 4.7d) are generally consistent with those of the marine deposits, except that ejecta samples show more uniform composition. Note that the hydraulically placed sandy fill was dredged from the original seabed, and hence has the same composition as marine deposits. The grading of the ejected soils is also consistent with the sand fractions of the fill material. Samples from the ejected soils were also collected from additional 15 locations (shown in Figure 4.6) by Tonkin+Taylor, on 14 November. Importantly, these samples were collected before the severe rainfall on 14-15 November (Greater Wellington Regional Council, 2017) that potentially washed out some of the fines fractions of the ejected soils. Grain size distribution curves of the gravelly samples and sandy samples collected on 14 November are shown in Figures 4.7a and 4.7b in the same fashion as Figures 4.7c and 4.7d. By and large, both gravelly samples (solid lines in Figure 4.7a) and sandy samples (solid lines in Figure 4.7b) are in good agreement with the respective range of grain-size distribution curves obtained from borehole samples (shaded areas). Tables 4.1.a and 4.1b summarize the field visual classification (Tonkin+Taylor, private communication), the mean grain size (D_{50}), and fines content (F_C) obtained from the laboratory tests on the samples collected on 14 November (Sample 1 to 15) and 17 November (S1 to S13) respectively.

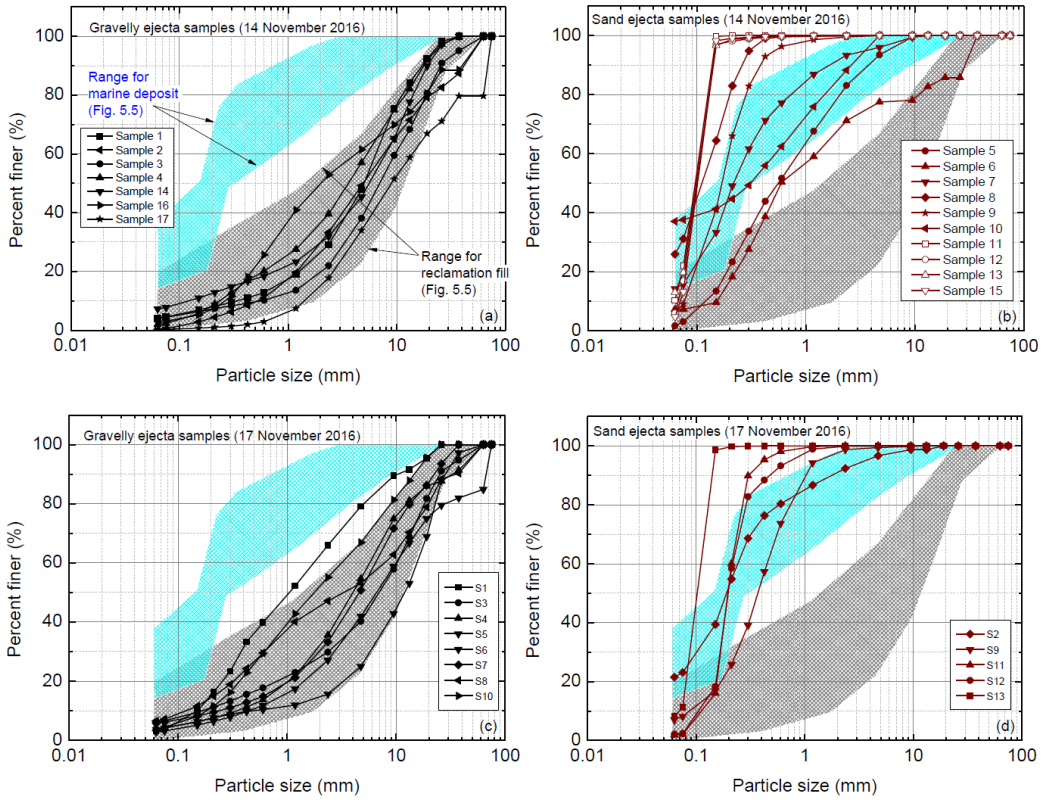

Figure 4.7: Grain size distribution for liquefaction ejecta samples collected on reclaimed land from (a) gravelly quarry rock fill on 14 November, and (b) sandy fill on 14 November, (c) gravelly quarry rock fill on 17 November, and (d) sandy fill on 17 November. Shaded regions show ranges of grain size for marine deposits and reclamation fill collected from subsurface explorations (plotted in Figure 2.5).

Table 4.1a: Field visual classification, fines content, and D_{50} of liquefaction ejecta samples collected on 14 November 2016.

Sample ID	D_{50} (mm)	Fines Content (%)	Field Visual Classification
Sample 1	5.12	4.51	Fine to coarse GRAVEL with trace sand, dark brownish grey. Saturated, poorly graded, angular, slightly weathered sandstone and mudstone, moderately strong. Sand is fine to coarse.
Sample 2	4.98	0.2	Fine to coarse GRAVEL with minor sand and cobbles, brown. Saturated, poorly graded, angular, moderately weathered sandstone and mudstone, moderately strong. Sand is medium to coarse.
Sample 3	6.98	4.09	Fine to coarse GRAVEL with minor sand and trace cobbles, dark brown. Wet, well graded, subrounded to angular, moderately weathered sandstone and mudstone, weak. Sand is coarse.
Sample 4	3.56	2.3	Fine to coarse GRAVEL with some sand, dark brownish grey. Wet, well graded, subrounded to angular, slightly weathered sandstone, moderately strong. Contains shell hash.
Sample 5	0.56	3.1	Fine to coarse SAND with trace gravel, dark brown. Saturated, poorly graded. Gravel is fine, subrounded.
Sample 6	0.41	9.6	Fine to coarse SAND with minor gravel, dark brownish grey. Wet, well graded. Gravel is fine to medium, subangular
Sample 7	0.22	15.9	Fine to medium SAND with minor silt and trace gravel, dark bluish grey. Saturated, poorly graded, dilatant. Gravel is fine to coarse, angular. Contains shell hash and wood fragments.
Sample 8	0.11	31.2	Silty, fine SAND, brown. Saturated, poorly graded, dilatant.
Sample 9	0.17	9.1	Fine to medium SAND, dark grey. Wet, poorly graded, dilatant. Contains shell hash.
Sample 10	0.31	35.6	Fine to medium SAND with minor gravel, bluish grey. Wet, poorly graded. Gravel is coarse, subrounded, slightly weathered sandstone, moderately strong. Contains shell hash.
Sample 11	0.096	21.9	Fine SAND, dark grey. Saturated, dilatant. Contains shell hash.
Sample 12	0.100	16.9	Fine SAND, dark grey. Saturated, dilatant. Contains shell hash.
Sample 13	0.098	19.7	Fine SAND, dark grey. Saturated, dilatant. Contains shell hash.
Sample 14	3.61	7.29	Fine to coarse GRAVEL with minor sand, brown. Wet, well graded, subrounded to angular, slightly weathered sandstone and mudstone, moderately strong to weak.
Sample 15	0.102	13.2	Fine SAND, dark grey. Saturated, dilatant. Contains shell hash.
Sample 16	2.00	2.75	Sandy, fine to coarse GRAVEL, brown. Wet, well graded, angular, moderately weathered sandstone and mudstone, weak. Sand is fine to coarse.
Sample 17	9.00	0.17	Fine to coarse GRAVEL with minor sand and trace cobbles, dark brown. Wet, well graded, subrounded to angular, moderately weathered sandstone and mudstone, weak. Sand is coarse.

Table 4.1b: Field visual classification, fines content, and D_{50} of liquefaction ejecta samples collected on 17 November 2016.

Sample ID	D_{50} (mm)	Fines Content (%)	Field Visual Classification
S1	1.08	3.1	Fine to coarse SAND with some gravel, dark grey. Moist, poorly graded. Gravel is subangular to angular, slightly weathered mudstone, moderately strong.
S2	0.19	21.5	Fine to coarse SAND, bluish grey. Moist, poorly graded. Contains shell hash.
S3	7.38	6.2	Fine to coarse GRAVEL with some sand and minor cobbles, dark brown. Moist, well graded, subangular to angular, moderately weathered sandstone and mudstone, moderately strong to weak. Contains shell hash.
S4	4.17	3.9	Fine to coarse GRAVEL with some sand and trace silt, dark brown. Wet, well graded, subangular to angular, slightly weathered mudstone, weak. Sand is fine to coarse.
S5	12.09	3.7	Fine to coarse GRAVEL with minor sand and cobbles, brown. Moist, well graded, subrounded to angular, moderately weathered sandstone and mudstone, moderately strong. Sand is fine to coarse.
S6	7.02	2.8	Fine to coarse GRAVEL with some sand and minor cobbles, dark brown. Moist, well graded, subangular to angular, moderately weathered sandstone and mudstone, moderately strong to weak. Contains shell hash.
S7	4.64	5.8	Fine to coarse GRAVEL with some sand, dark brown. Moist, well graded, subangular to angular, moderately weathered sandstone and mudstone, moderately strong to weak.
S8	3.51	6.5	Fine to coarse GRAVEL with some sand and minor cobbles, dark brown. Moist, well graded, subangular to angular, moderately weathered sandstone and mudstone, moderately strong to weak.
S9	0.37	7.0	Fine to coarse SAND with trace gravel and silt, brownish grey. Moist, poorly graded. Gravel is fine to medium, angular, moderately weatheredemudstone, moderately strong.
S10	1.87	3.9	Sandy, fine to coarse GRAVEL, brownish grey. Moist, well graded, subangular to angular, moderately weathered sandstone and mudstone, moderately strong to weak. Sand is fine to coarse.
S11	0.20	1.9	Fine to medium SAND, dark grey. Moist, poorly graded. Contains shell hash.
S12	0.20	2.1	Fine to medium SAND, dark grey. Moist, poorly graded. Contains shell hash.
S13	0.11	8.3	Fine SAND, dark grey. Saturated, poorly graded, dilatant.

4.3 Settlement

Differential hand-measured vertical settlement measurements are summarized in Figure 4.8. These measurements are of ground settlement relative to pile supported structures. Settlement of fill relative to buildings supported on a shallow foundation are excluded from this figure. The settlement of the fill south of the Old Seawall is generally in the range from 300 mm to 500 mm, whereas settlement of the order of 100 mm to 200 mm was observed in the hydraulic fill north of the seawall. The largest settlement was observed at the Thorndon Container Terminal just behind the wharf where a vertical offset of about 600 mm was observed. Approximately 180 meters inland of the Thorndon Wharf bulkhead, 180 mm of settlement were measured relative to what appeared to be the piles of the historic gantry crane at North Rail (see Figure 2.2).

4.4 Lateral spreading

Lateral spreading generally was manifested by typical cracks and fissures on the pavement surface running perpendicular to the direction of spreading. Characteristic spreading-induced movements are illustrated for the Thorndon Container Terminal (TCT) in this section, whereas additional observations on lateral spreading are discussed in the subsequent sections on wharves and buildings.

To quantify the magnitude and spatial distribution of lateral spreading at TCT, lateral spreading measurements were performed by ground surveying along two transects in the east-west direction, denoted as TCW-1 and TCW-2 in Figure 4.9. Along each transect, ground cracks were identified and their location (horizontal distance from a reference point) and width were recorded. By summing up the crack widths one can estimate the size of lateral ground displacements as a function of the distance inland from the wharf, as illustrated in the plot shown at the top of Figure 4.9. Note that along TCW-2 two independent transects were performed approximately 10 m apart (in the N-S direction) to check the accuracy in the estimates of ground displacements. Table 4.2 lists the width and horizontal distance to each crack from the reference point of each transect. The cumulative opening of the cracks measured across TCW-1 and TCW-2 are 960 and 785 mm, respectively, implying that the edge of the fill moved laterally towards the sea (Thorndon Wharf) about 0.8 m to 1.0 m.

The lateral spreading was accompanied by a typical slumping mode of deformation involving lateral expansion and associated vertical settlement. Ground settlement immediately inland of the bulkhead, relative to the wharf deck, was estimated to be 600 mm, as indicated in Figure 4.9. Further details on the vertical offsets and settlement induced by the liquefaction and lateral spreading are described in Chapter 6 where observations on the Thorndon Wharf are provided.

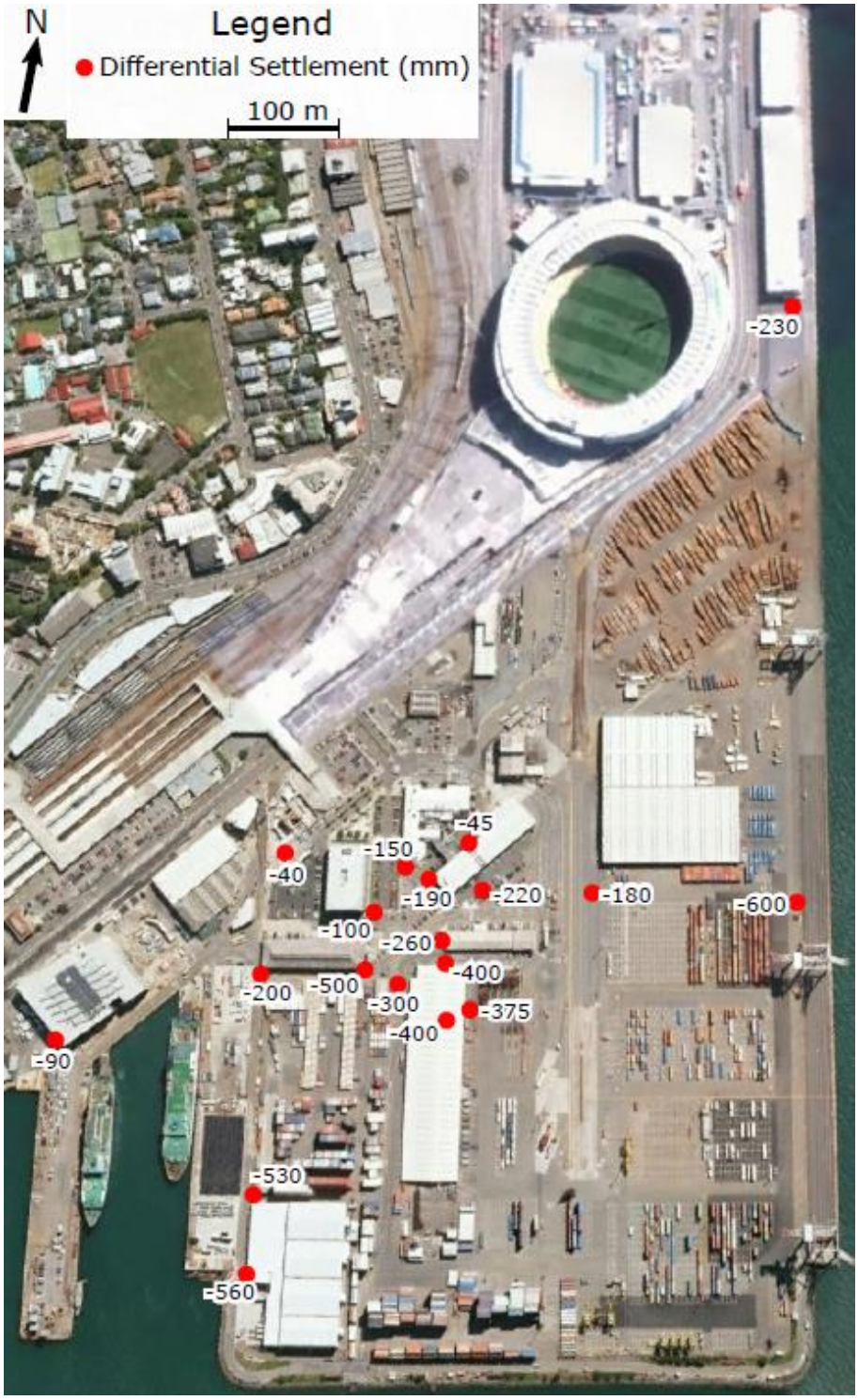

Figure 4.8: Location and magnitude of differential settlement measurements obtained during inspections. All values are in mm, and represent settlement of the ground surface relative to a pile supported structure. (Base image from Google Earth™)

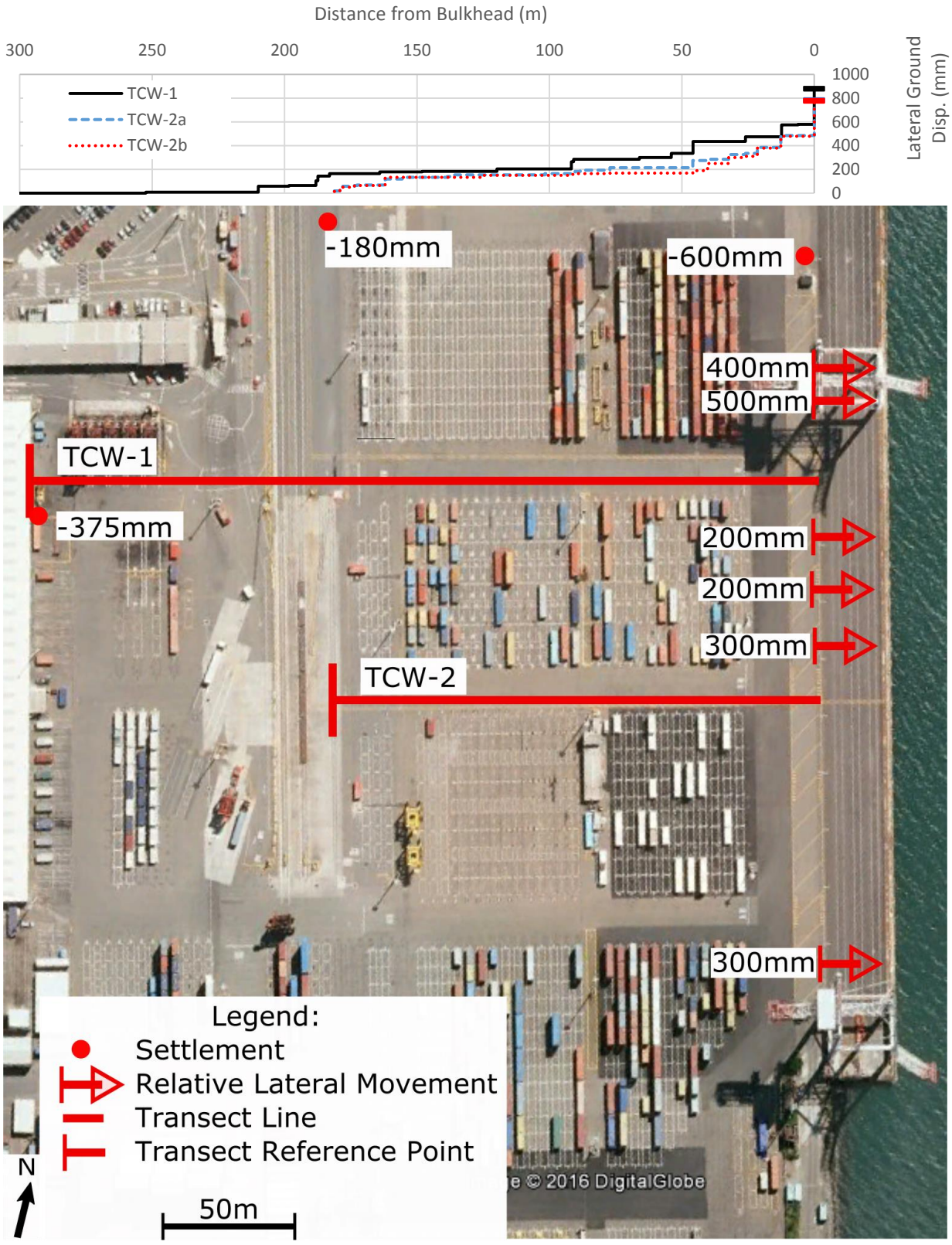

Figure 4.9: Location of west-to-east transects for lateral spreading measurements towards Thorndon Wharf during inspections. Plots at the top show cumulative lateral ground displacement versus horizontal distance from the bulkhead. Transect measurements are in Table 4.2. (Base image from Google Earth™)

Table 4.2: West-to-east lateral ground displacement measurements toward Thorndon Wharf.

TCW-1		TCW-2		
Horizontal Distance from Reference Point (m)	**Crack Width (mm)**	**Horizontal Distance from Reference Point (m)**	**Crack Width[1] (mm)**	
48.80	10	0.00	20	15
91.30	50	2.14	35	35
102.90	5	3.32	5	–
113.00	40	7.62	5	15
113.80	40	8.50	5	–
118.20	20	19.20	50	70
137.10	15	25.60	5	–
153.20	5	26.75	10	–
181.40	20	42.65	5	–
209.50	60	45.45	15	–
210.30	20	55.55	–	15
235.20	15	79.45	10	10
247.20	35	89.95	5	5
255.40	100	90.85	15	5
275.20	40	92.8	10	–
288.8	100	104	20	20
295.1	5	135.3	60	60
301.20	300	140.9	10	–
48.80	10	148.9	40	50
–	–	155.20	10	10
–	–	159.70	50	70
–	–	168.60	100	100
–	–	181.20	300	300
Total:	880	Total:	785	780

1) Two measurements were taken approximately 10 m apart (North to South)

5. LIDAR FIELD SURVEY AND DATA PROCESSING

5.1 Background

Terrestrial laser scan (TLS) surveys (also known as ground-based LiDAR) were completed at CentrePort from 28 November to 1 December 2016 to document the ground and structural performance during the 2016 Kaikoura earthquake. The primary purpose of the surveys was to collect TLS data to supplement and validate structure from motion (sfm) point clouds from recent UAS surveys. As such, TLS data were collected along North/South and East/West transects across the site, and around and on the inside of several key structures. Most scans were conducted outside; however, scans were completed in three buildings (i.e., CPH, S37, and CS buildings).

The surveys were completed using a Leica P40 terrestrial laser scanner with a Leica GS14 GNSS receiver mounted above (Figure 5.1) at a calibrated offset of 0.1580 m. Scans were spaced generally at 30-40 m apart along transects (Figure 5.2); however, the spacing varies substantially to accommodate visibility constraints as well as safety considerations on the operating port facility. Scans were completed for a 360 degree panoramic view. Most scans also have co-acquired, high resolution imagery utilizing the internal calibrated camera in the P40 scanner. The camera captured over 270 (1920x1920) images for the full dome and mosaics and blends them together to map colors to the point cloud. For some of the indoor scans with poor lighting conditions or where scans needed to be completed rapidly, the camera imagery was not acquired. For indoor scans, the GNSS receiver and handle were removed prior to scanning, in most cases, for full overhead scanning. A second GNSS receiver was utilized as a base station over a control point (CARDNO 19) for one of the scan dates. For the other days a local Continually Operating Reference Station (CORS) WGTT was utilized as the base station.

Figure 5.1: Example scan setup with a Leica P40 terrestrial laser scanner and Leica GS14 GNSS receiver mounted directly above the scanner.

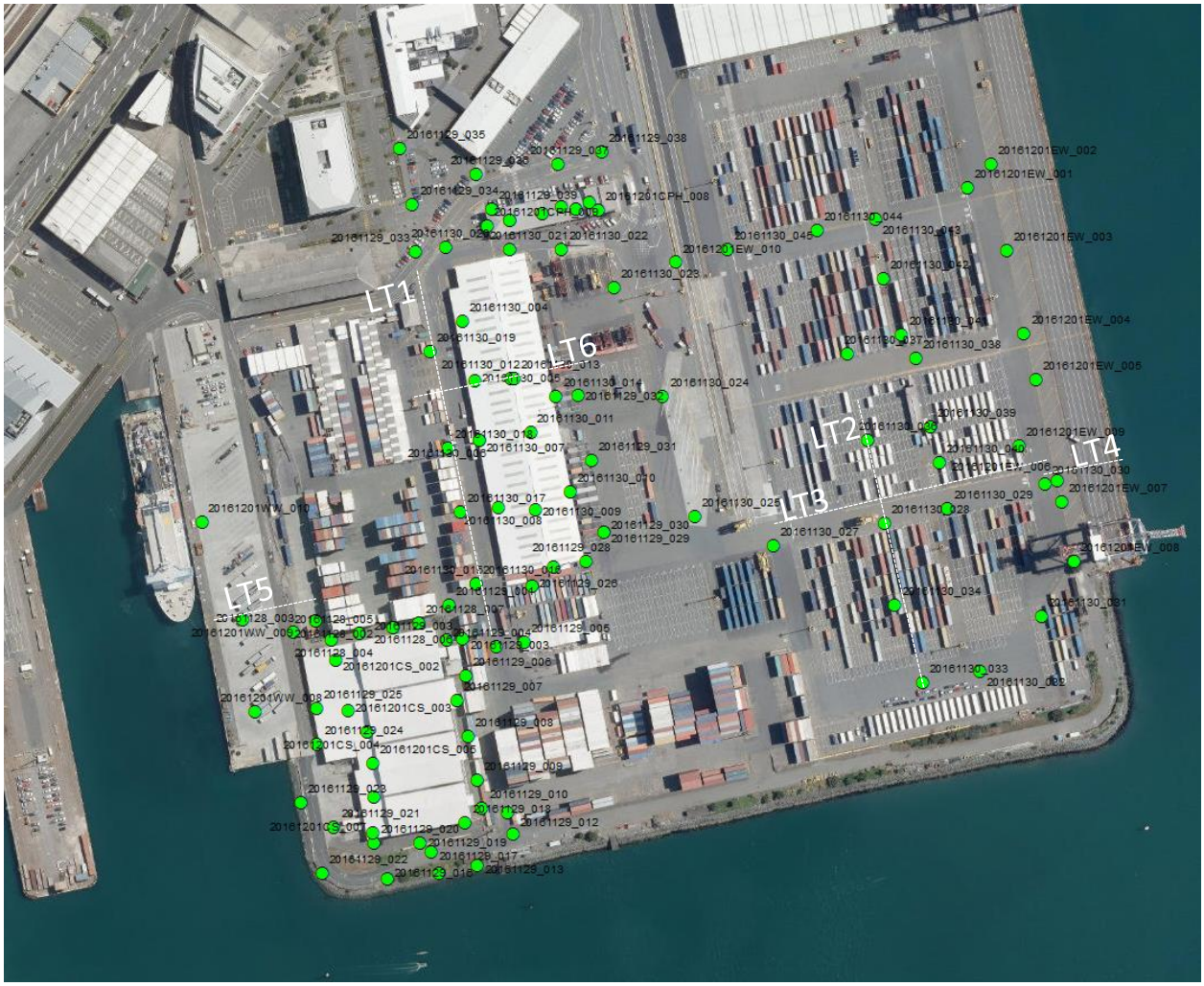

Figure 5.2: Locations (green circles) where terrestrial laser scans were obtained at the CentrePort. Additional scans were captured inside the Cruise Ship Terminal to the North that are not shown on the map because they are being processed. Transects from the LiDAR data shown later in the report are identified. Note that the basemap is from ESRI prior to the earthquake.

This document assumes the reader has a basic knowledge of TLS and its use in reconnaissance. Additional background on TLS can be found in Kayen et al. (2010), Olsen and Kayen (2012), and its use in similar type reconnaissance is well documented in multiple GEER reports (http://www.geerassociation.org/).

5.2 GNSS processing

A local CORS, WGTT (http://apps.linz.govt.nz/gdb/index.aspx?code=WGTT), was utilized as the reference for all Global Navigation Satellite System (GNSS) processing to provide geo-referenced coordinates to all of the TLS data acquired. However, the current published coordinates for WGTT are pre-earthquake coordinates, which do not account for the earthquake-induced deformations (Figure 5.3). Hence, RINEX files for the four dates of

survey were post-processed in *PositioNZ* using other CORS in the network. The resulting coordinates were subsequently averaged to obtain post-earthquake coordinates (January 6, 2017). *PositioNZ* has updated the positions of CORS to post-earthquake coordinates (and updates those on a daily basis).

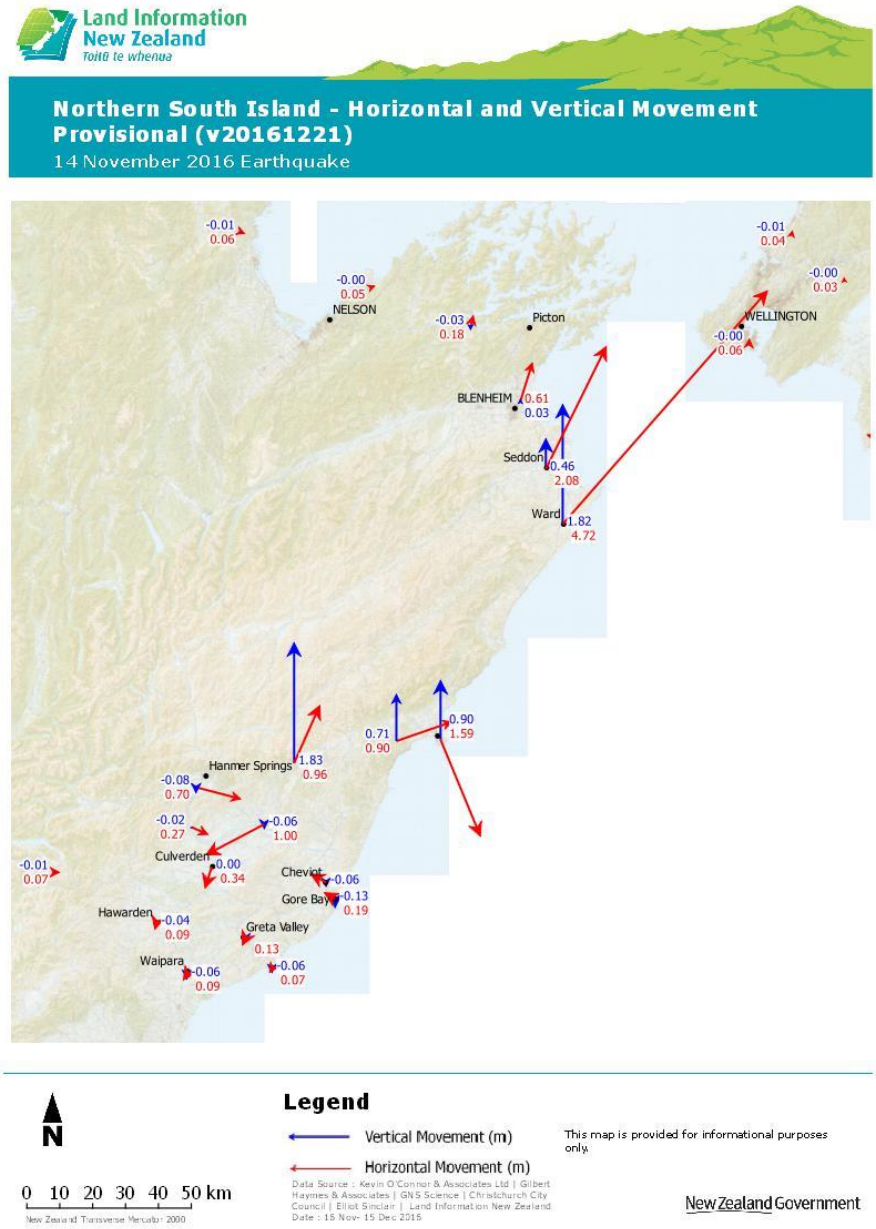

Figure 5.3: Estimated earthquake displacements at CORS (Source: LINZ).

GNSS baselines to scan locations were post processed in Leica GeoOffice v8.4 using WGTT as the reference station. The resulting 3D (Earth Centered Earth Fixed, ECEF) coordinates were then converted to the coordinate system in Table 5.1 using the LINZ online coordinate conversion tool. A summary of the coordinate system and reference datums used for the survey is in Table 5.2.

A temporary base station was set up on point CARDNO 19 on 11/30/2016 for a portion of the LiDAR survey. This station was used as a check against the data processed with the WGTT CORS. The coordinates were consistent to less than 1 cm. Additional checks against CARDNO control points were completed and were consistent within 1 cm after accounting for general differences in pre/post-earthquake coordinates. Coordinates for these points were extracted directly from the scans.

TLS scans were import into Leica Cyclone 9.1.4. On import, saturated pixels were removed (highly reflective objects at close range that result in incorrect coordinates) in addition to moderate mixed pixel removal (locations where the light is split between objects too close to distinguish) to minimize noise present in the point clouds.

Table 5.1: Post-earthquake coordinates utilized for CORS WGTT compared with the pre-earthquake results.

Coordinate	Easting (m)	Northing (m)	Elevation (m)	ΔE# (m)	ΔN# (m)	ΔElev# (m)
Pre-Earthquake* (Published)	400436.134	801185.183	30.316	-	-	-
Pre-Earthquake (PositioNZ)	400436.139	801185.184	30.319	0.005	0.001	0.003
Post-Earthquake (PositioNZ)	400436.153	801185.264	30.308	0.019	0.081	-0.008

**Pre-earthquake coordinates are Wellington Circuit 2000, NZGD2000, defined at nominal epoch 2000.0 with deformation model version 20160701.*

#Differences in Easting, Northing, and Elevation are relative to the published coordinates.

Table 5.2 Summary of Coordinate System and reference datums utilized for the survey.

Horizontal Datum:	New Zealand Grid Datum 2000 (NZGD 2000)
Datum Version:	v20160701
Vertical Datum (Heights):	Wellington 1953 (NZVD 2016)
Circuit\Projection:	Wellington Circuit 2000
Coordinate Epoch:	20161129 (Observation Date(s): 11/28-12/1, 2016)
Coordinate Source:	PositioNZ-PP, Processed 1/X/2017

5.3 TLS registration

During the survey, pivoting 114-mm diameter black and white pattern targets with a metallic base were utilized to provide tie points between scans. These targets can be rotated to provide ideal incidence with the scanner from each scan position while ensuring that the center remains in the same location. The targets were strategically moved throughout the scanning

process. Additional 152-mm diameter black and white pattern targets printed on durable label paper were utilized for some locales to provide additional tie points.

Center points for these targets were extracted using fitting algorithms in Leica Cyclone 9.1.4 software. These points were then used to build a preliminary registration. In some locales where there were insufficient targets, visual registration processes to approximately register two scans were followed by cloud-to-cloud surface matching. Cloud-to-cloud constraints were then added for significantly overlapping scans and added as additional constraints in the registration. These additional constraints help improve results at farther angles. A reference target was placed at the origin of each scan and linked to GNSS coordinates obtained for most scan origins.

A weighted, least-squares adjustment was utilized using all scans and constraints to determine the appropriate transformations (translations and rotations) for each scan. The following weights were utilized for this registration: 1.0 for targets that were clearly visible in each scan, cloud-to-cloud matches between close scans with substantial overlap, and GNSS coordinates for scan origins; 0.5 for targets of lower confidence; 0.3 for cloud-to-cloud matches between scans with some overlap but spaced further; and 0.2 for some GNSS coordinates of lower, but still acceptable, quality due to visibility obstructions. Periodically, distant features (e.g., light poles) visible in many scans across the port were utilized for quality control. Some GNSS coordinates with high residuals were removed in areas with very poor sky visibility due to the narrow pathways between shipping containers. The 3D weighted mean absolute error for all of the constraints was 0.0026 m. RMS differences between scan pairs for cloud-to-cloud registrations were typically less than 0.015 m.

Following the registration, a variety of quality control checks were implemented in addition to statistical analysis. These include coloring each scan a unique color and verifying the dataset was free of significant offsets between scans in cross sections.

5.4 DEM creation

Preliminary Digital Elevation Models (DEMs) were created across CentrePort. Refined models are in the process of being created. The following process was utilized:

1. The registered point cloud of the port was segmented into distinct geographic regions with overlap for processing efficiency.
2. Point clouds for each section were manually cleaned to remove building exteriors, walls, shipping containers, noise, and artificially low points resulting from multipath effects of the laser from wet or highly reflective surfaces. Lower level floors of buildings were left in the models to include in the DEMS.
3. The point clouds were then processed further in a custom ground filtering algorithm to remove additional spurious points.
4. The data were then organized into spatial bins of 0.05 to 0.10 m (depending on location).
5. Small holes were filled using a roving thin plate spline (see Olsen et al. 2015).

6. The data were then triangulated using the approach of Olsen et al. (2015) to create a DEM.
7. Derivative products such as slope maps and hillshades were then created for the DEMs to highlight discontinuities.
8. The resulting DEMs were used for settlement analyses as well as for generating cross sections.

Figure 5.4 shows a cross-section obtained on the west edge of the road immediately west of Building S37. The peaks are locations of the buried piles and the lower portions are settlement of the pavement surface around those piles. In absence of detailed survey data prior to the event, the original surface was estimated by fitting a 3rd order polynomial (R^2 = 0.99) to the tops of piles with higher elevations in the local area. Given this assumption, the differential settlement calculations (Figure 5.4(b)) do not account for any settlement of those piles which may have occurred given that some of the piles in that sequence appear to have settled. Regardless, the trends are reasonably consistent with the values shown in Figure 4.8.

Several TLS observations were obtained throughout the area surrounding the CS building at the southwest corner of the port, which experienced widespread liquefaction-induced ground deformations. The LiDAR DEM was converted to a hillshade to enhance visualization of cracks and other features in this area (Figure 5.5). The hillshade visualization highlights discontinuities in the data and provides detailed information on cracking patterns observed. In addition, differential settlement between the concrete slabs between the road and cold store building are apparent.

Figure 5.6 presents example DEMs with perspective views. From the LiDAR scans, significant differences in elevation from liquefaction are apparent. Figure 5.7 presents two cross-sections through this locale, one running north to south (Figure 5.7(a)) and one running west to east (Figure 5.7(b)). Although the pre-event surface was not available for comparison, it is likely that settlement increases significantly towards the south as a result of the increased liquefaction-induced ground spreading towards the south and west.

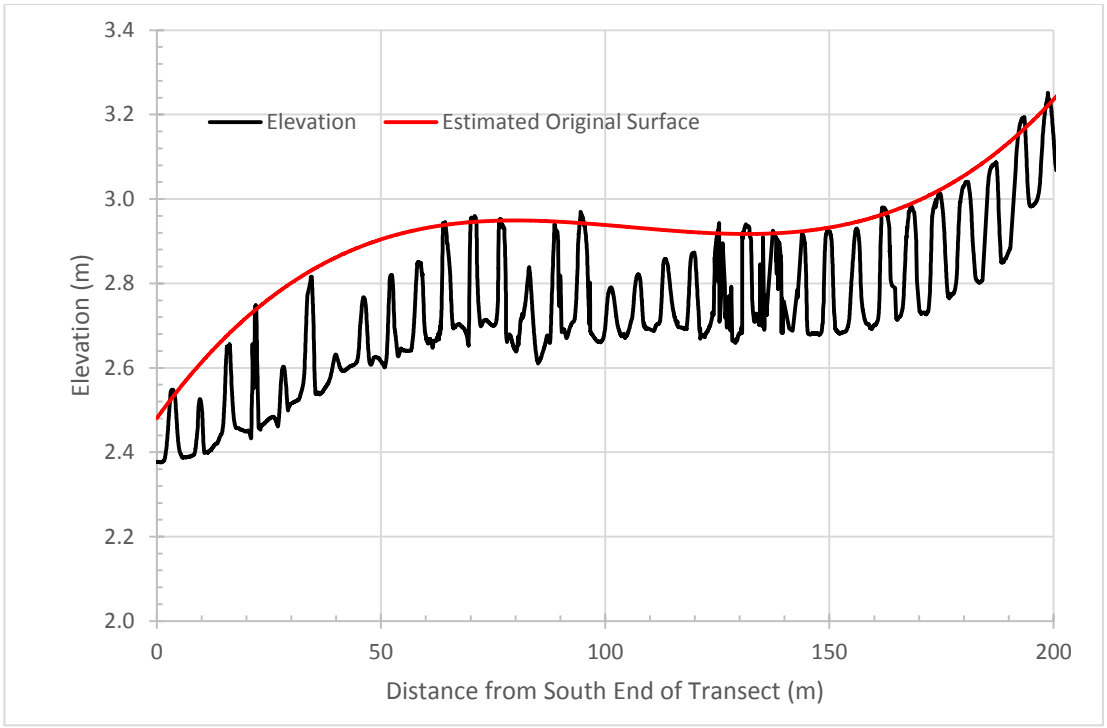

(a)

(b)

Figure 5.4: (a) Post-earthquake elevations for transect (LT1) along west side of roadway west of S37; the red line represents the estimated pre-elevation surface. (b) Estimated settlements. (Distance 0 is approximately 15 m south of the south wall of Building S37 and the 200 m transect runs to about 3 m north of the north wall of Building S37).

Figure 5.5: Example hillshade for the SW corner of the port, south of the CS building. This dataset was coarsely cleaned and still contains several artifacts from railing and metal racks.

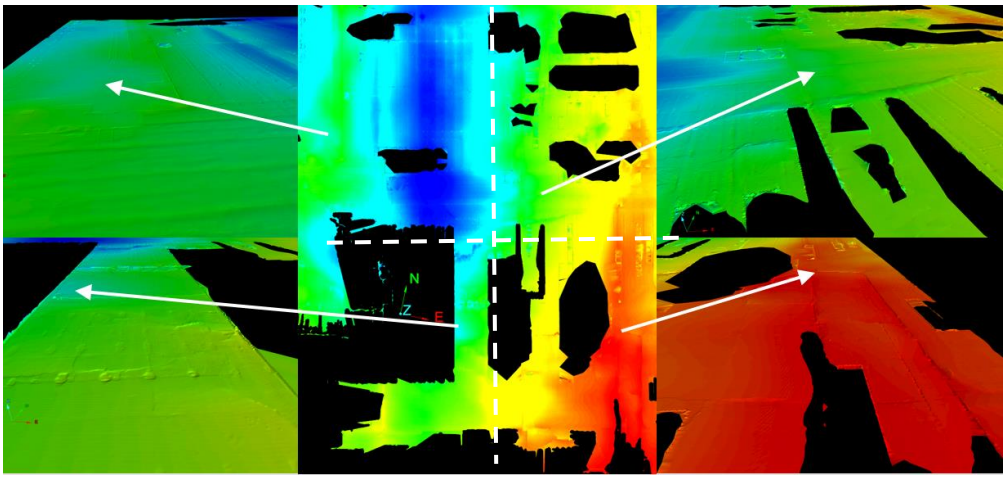

Figure 5.6: Example DEMs of the southeast portion of the port (next to, but not including Thornton Wharf) highlighting various liquefaction settlements and accretion of materials. Elevation ranges from 2.05 m (Red) to 3.80 m (Blue). The center image is a plan view, and the other images are perspective views to show detail.

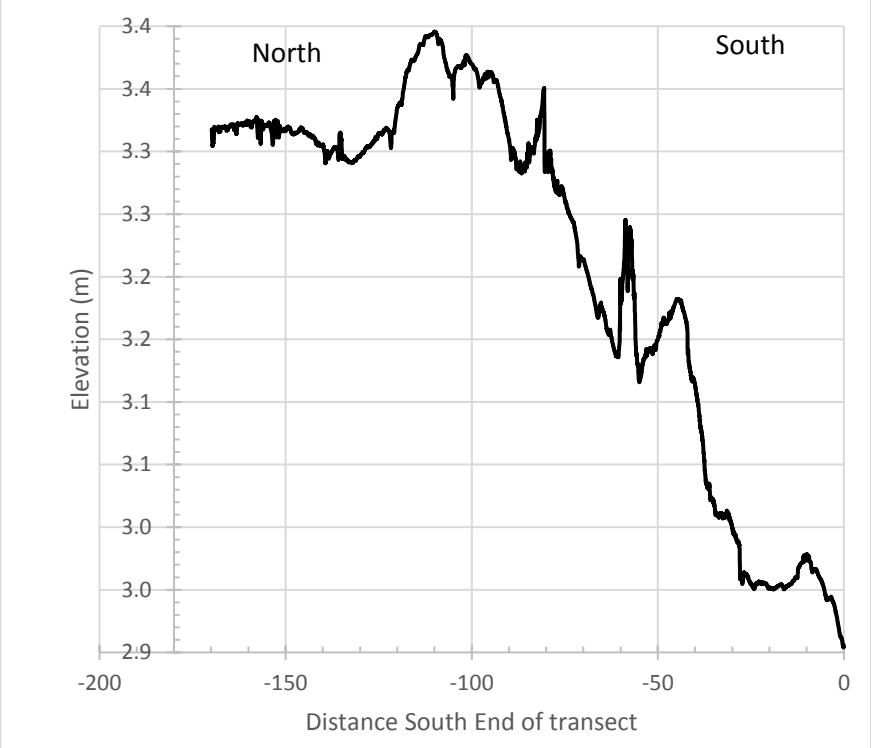

(a)

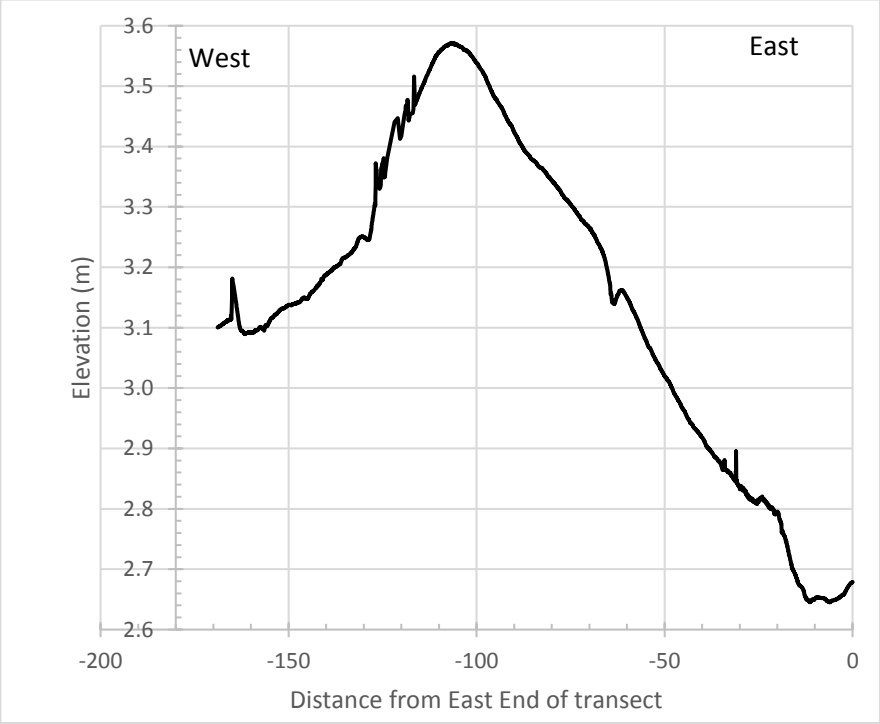

(b)

Figure 5.7: Cross sections across the southeast portion of the Thorndon Reclamation: (a) North South Transect LT2, and (b) East-West Transect LT3. Locations of transects are identified in Figure 5.2.

6. EFFECTS ON WHARVES

6.1 General

CentrePort Limited has Thorndon Container Wharf and King's Wharf. Figure 6.1 is a plan view of the port showing the location of the two wharf structures. The port's primary container operation takes place on Thorndon Container Wharf, which is on the eastern side of the port. King's Wharf, which is on the western side of the port, supports primarily roll-on/roll-off cargo.

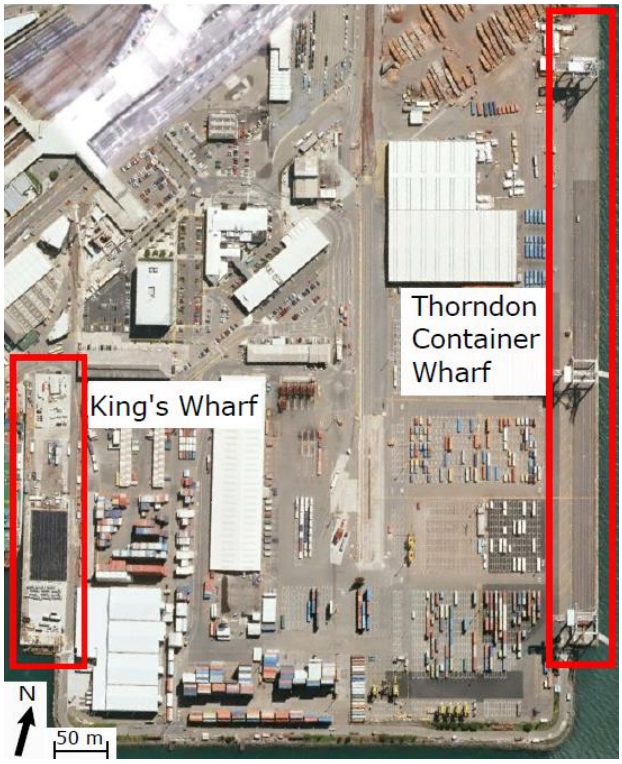

Figure 6.1: CentrePort Wellington map identifying the two wharves documented in this report. (Base image from Google Earth™)

6.2 Thorndon Container Wharf

The Thorndon Container Wharf is supported on 7 rows of 508x508-mm square, pre-stressed concrete piles. Pile bents are spaced 3.66 m on center or at approximately $s = 6B$. The piles are generally 18 m long under the eastern crane rail and 20 to 23 m long (increasing in length to the south) under the western crane rail (Tonkin & Taylor Ltd. 2012). Widespread liquefaction of the Thorndon Reclamation (Figures 6.2, 4.1 and 4.2) was accompanied with settlement of the fill and lateral spreading towards Thorndon Wharf. As described in Chapter 4, the lateral spreading displacements at the edge of the fill (bulkhead) reached about 0.8 m to 1.0 m (Figure 4.9 and Table 4.2). The lateral thrust from the displaced fill pushed the inland piles of the wharf causing tilt of the wharf. The crane rail tilted 2.5° down towards the sea at TWC-1 and 1° down towards the sea at TWC-2 (see Figure 4.9 for transect locations). Lateral seaward movement measurements of the bulkhead relative to the ground immediately inland

of it are listed in Table 6.1 and indicated in Figure 4.9. These measured values range from 200 to 500 mm. Ground settlement immediately inland of the bulkhead, relative to the wharf deck, was estimated to be 600 mm. Figures 6.3 and 6.4 show the vertical offset created between the pile supported wharf and reclaimed fill behind the wharf.

The QuakeCoRE-GEER team was informed that concrete piles had been sheared near the pile cap (from a boat survey by others; T+T (2016) private communication). From the south side of the port, the QuakeCoRE-GEER team did observe a vertical bulkhead pile sheared just below the pile cap (Figure 6.5a). During a site visit in May 2017, the team observed that the bulkhead piles (both plumb and battered) near the north end of the Thorndon Reclamation were damaged immediately below the deck (Figure 6.5b). Cardno performed an aerial survey of the port that captured vertical settlement and lateral movement, which is shown in Figure 6.6.The magnitude of lateral spreading displacement and settlement measured by Cardno are generally consistent with those measured by the QuakeCoRE-GEER team, which are provided in this report.

Figure 6.7 shows the LiDAR-derived DEM for the Thorndon Wharf and surrounding terrain. The wharf deck has substantial concavity as observed in the cross section in Figure 6.8. Differential settlements between the wharf deck and adjacent pavement ranged from 435 mm to 780 mm, generally increasing towards the North. Figure 6.9 provides a close up of ejecta and offsets at the northern end of this portion of the wharf.

Figure 6.2: Widespread liquefaction of gravelly end-dumped quarry rock reclamation in container stacking area inland of Thorndon Wharf (S41.276608° E174.786309°, taken on 21NOV16)

Table 6.1: Estimates of seaward movement of bulkhead relative to inland soil.

TWC Station	Seaward Separation at Bulkhead (mm)
40+00	300
160+00	300
180+00	200
200+00	300
250+00	500
260+00	400

Figure 6.3: Looking south along Thorndon Wharf bulkhead at approximately STA 240. Approximately 600 mm of ground settlement measured relative to pile-supported wharf. (S41.278250° E174.789205°, taken at 1124 hrs on 21NOV16)

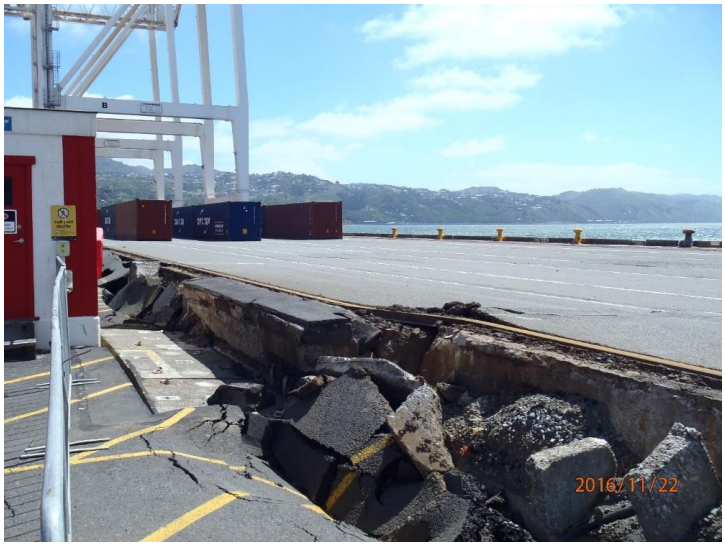

Figure 6.4: Looking north along Thorndon Wharf bulkhead at approximately STA 280. Approximately 600 mm of ground settlement measured relative to pile-supported wharf. (S41.277743° E174.789236°, taken on 22NOV16)

(a)

(b)

Figure 6.5: (a) Looking north towards the southern end of Thorndon Wharf. The vertical bulkhead pile is sheared just below the pile cap. QuakeCoRE-GEER team was informed that many piles in this area were sheared near the pile cap (from a boat survey by others; T+T (2016) private communication) (S41.280219° E174.789974°, taken at 1152 hrs on 22NOV16) (b) Looking north under the Thorndon Wharf bulkhead toward damaged plumb and battered bulkhead piles. (S41.277312° E174.789081°, taken at 13:38 hrs on 08MAY17)

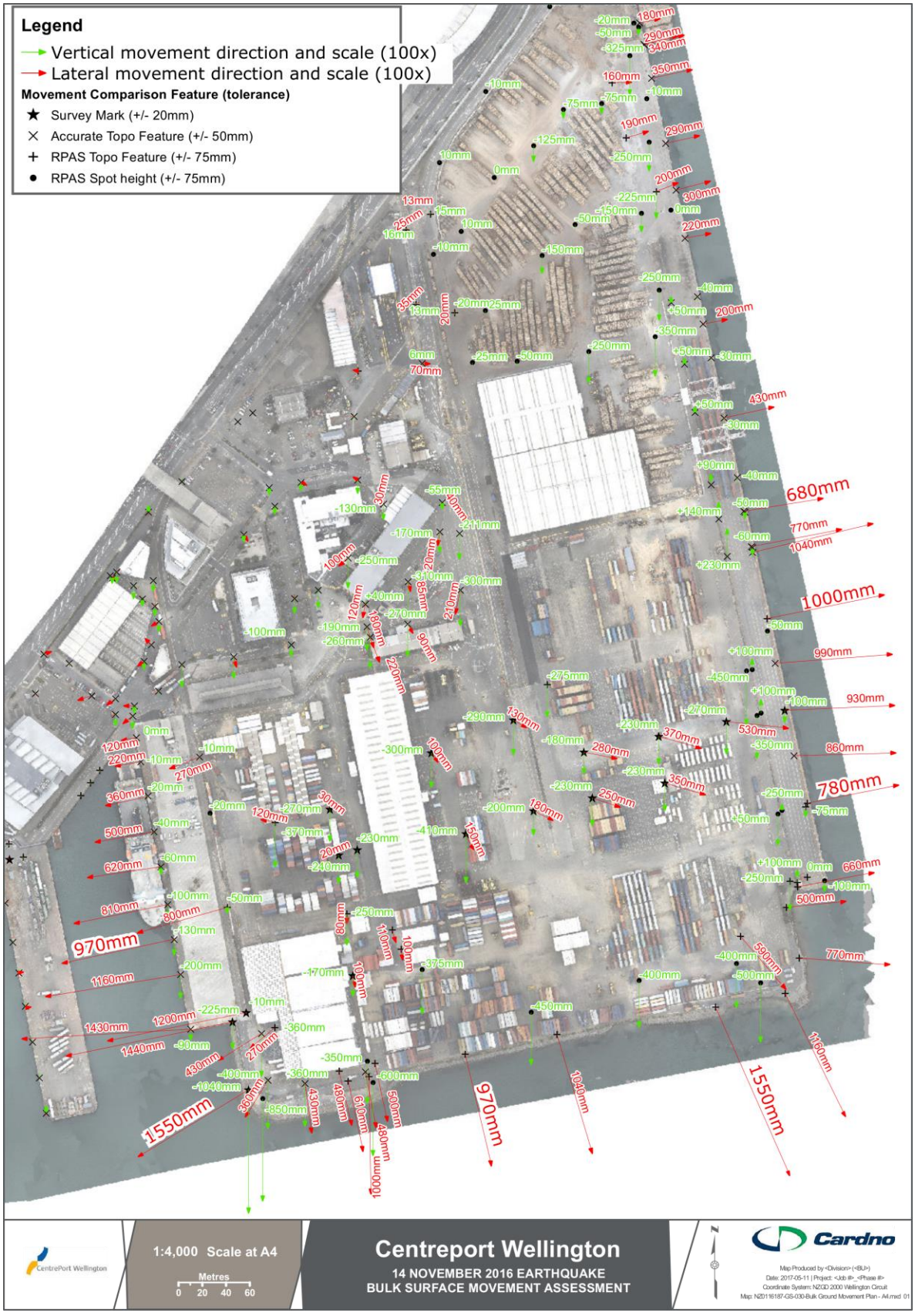

Figure 6.6: Aerial survey of Thorndon Reclamation and Wharf (performed by Cardno).

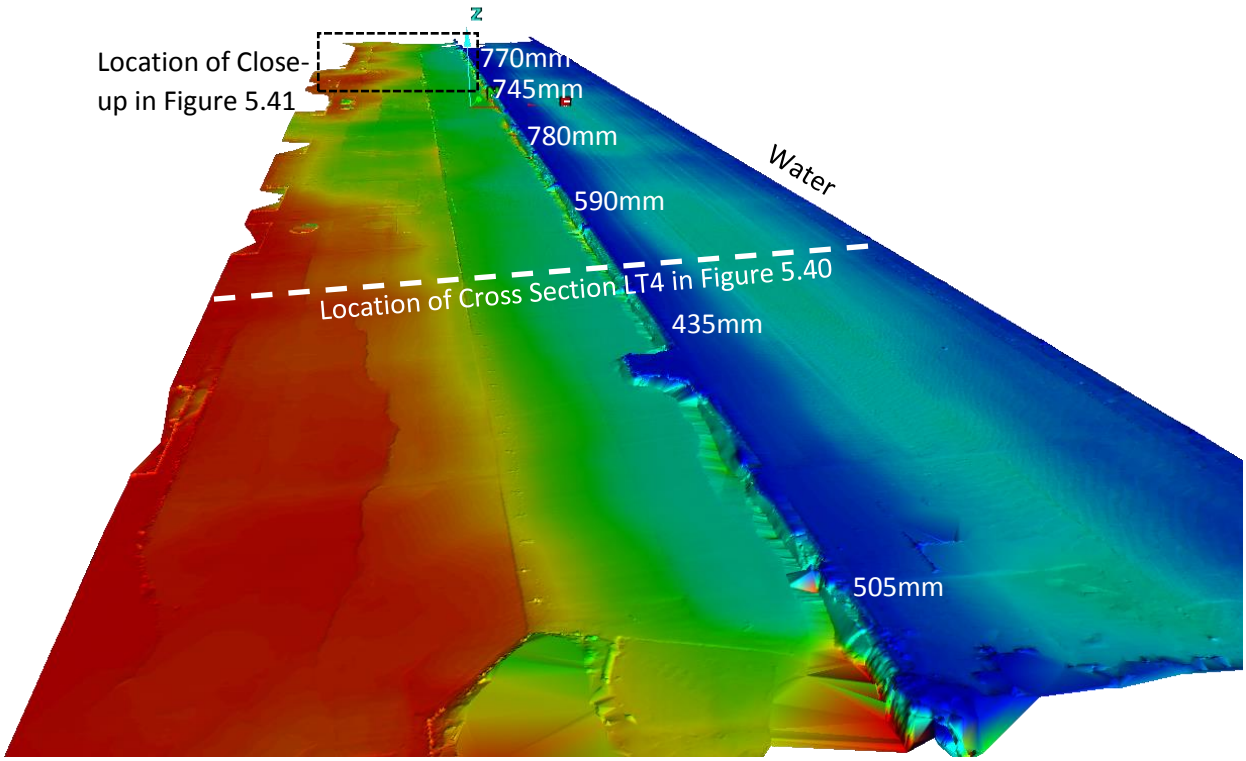

Figure 6.7: Perspective view of the LiDAR DEM of the eastern section of the port looking northward including the Thorndon Wharf and surrounding area colored by elevation to highlight discontinuities from cracks. Elevation ranges from approximately 2.60 m (red) to 3.60 m (dark blue). Differential settlements between the Wharf and Port are identified.

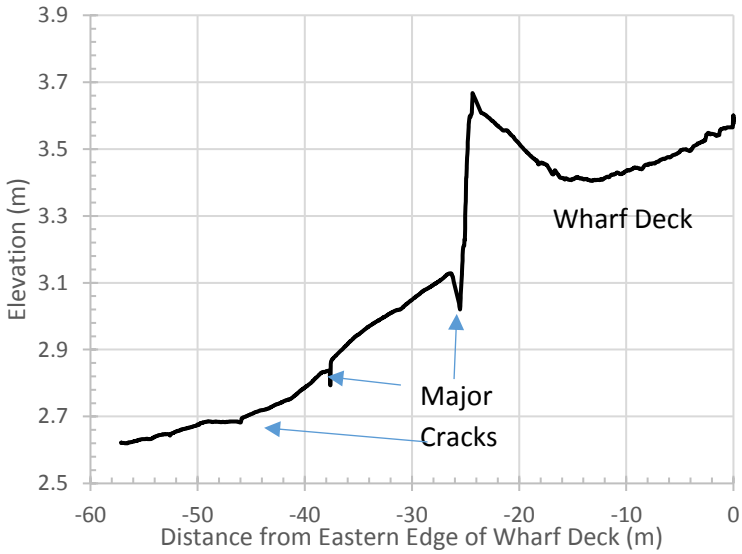

Figure 6.8: Elevation profile for cross section LT4 across Thorndon Wharf and inland fill. The location of the cross section is shown in Figure 6.7.

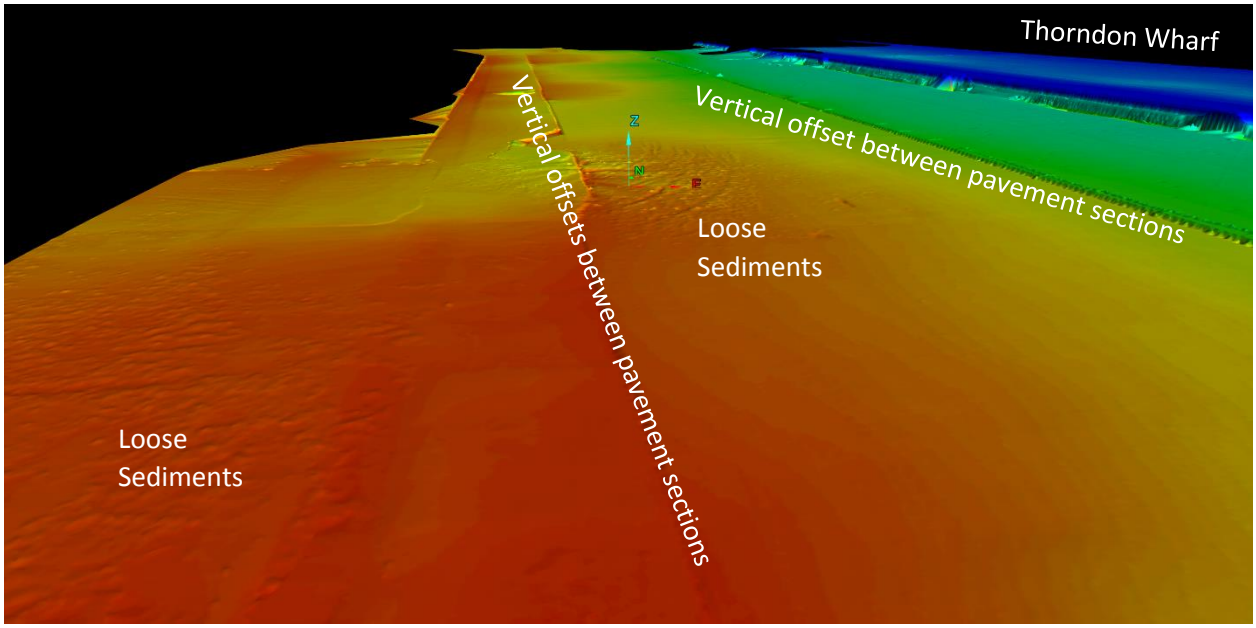

Figure 6.9: Close-up of the port surface highlighting cracking and separation between asphalt sections as well as loose sediments from ejecta (rougher sections of DEM) in the vicinity of Thorndon Wharf (see Figure 6.7).

6.3 King's Wharf

King's Wharf is supported on driven timber piles. The fill behind the wharf liquefied and moved laterally towards the wharf (sea) displacing King's Wharf to the west. The spreading displacement was the largest at the south end of the wharf where based on our lateral spreading measurements the lateral movement of soils behind the wharf exceeded 1.1 m. The ground along the edge of the reclamation displaced westward (towards the wharf) and downwards (beneath the wharf deck) as illustrated in Figure 6.10 (and Figure 7.8). The ground settlement relative to the deck of the wharf was approximately 560 mm at the southeast corner of the wharf (Figure 6.10) and 530 mm at the northwest corner of the CS building (Figure 7.8). Ground movements in the vicinity of the CS building (S41.28105° E174.78483°) near the southern end of King's Wharf were measured and are listed in Table 7.1 for Transects CS-1, CS-2, and CS-6, which will be presented and discussed later in the report. Note that the magnitude of spreading displacements generally decreased towards the north section of the wharf.

The inland timber piles split due to seaward (westward) lateral movement of the deck relative to the piles (Figure 6.11). Westward movement of the structure is visible in Figure 6.12, in which the southern row of piles is shown leaning to the west. Some vertical curvature of the wharf deck can be observed in the LiDAR DEM (Figure 6.13) and associated cross section in Figure 6.14. Differential settlement between the wharf and adjacent ground range from 475 mm to 630 mm as measured from the LiDAR-derived DEM. The wharf deck exhibits significant concavity (downward) as observed in the cross section plotted on Figure 6.14.

Figure 6.10: Looking North along bulkhead of King's Wharf. Approximately 560 mm of ground settlement relative to deck at southeast corner of King's Wharf. The west wall of the Cold Store shed is visible to the right of the photograph. (S41.281142° W174.784444°, taken at 1416 hrs on 21NOV16)

Figure 6.11: Looking under King's Wharf at an inland bulkhead pile. Timber pile is split from lateral movement (seaward/westward) of the deck relative to the pile. (S41.280900° E174.784375°, taken at 1412 hrs on 21NOV16)

Figure 6.12: Looking west along southern end of King's Wharf. Westward tilt of piles is visible. (S41.281281° W174.784097°, taken on 17NOV16)

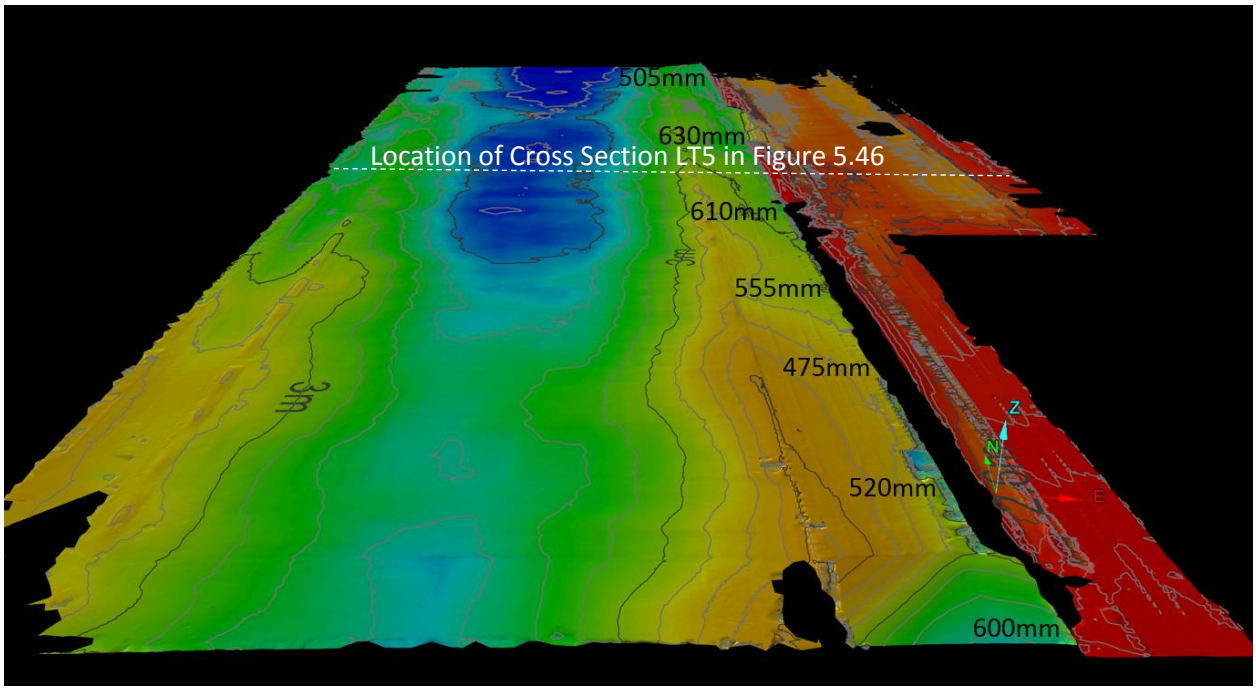

Figure 6.13: Perspective view of the LiDAR derived DEM (looking northward) of the pile supported King's Wharf showing measurements of differential settlement the adjacent ground. Elevation ranges from approximately 2.50 m (red) to 3.30 m (dark blue)

Figure 6.14: Cross section LT5 taken across King's Wharf and the adjacent ground based on LiDAR data shown in Figure 6.13.

7. EFFECTS ON BUILDINGS

7.1 General

Several engineered structures located on or adjacent to CentrePort Wellington were affected by the liquefaction-induced ground movements at the port. A few buildings were supported on shallow foundations. Most buildings were supported on pile foundations. Detailed reconnaissance observations for each building are presented in the following sections. Buildings are identified in Figure 7.1.

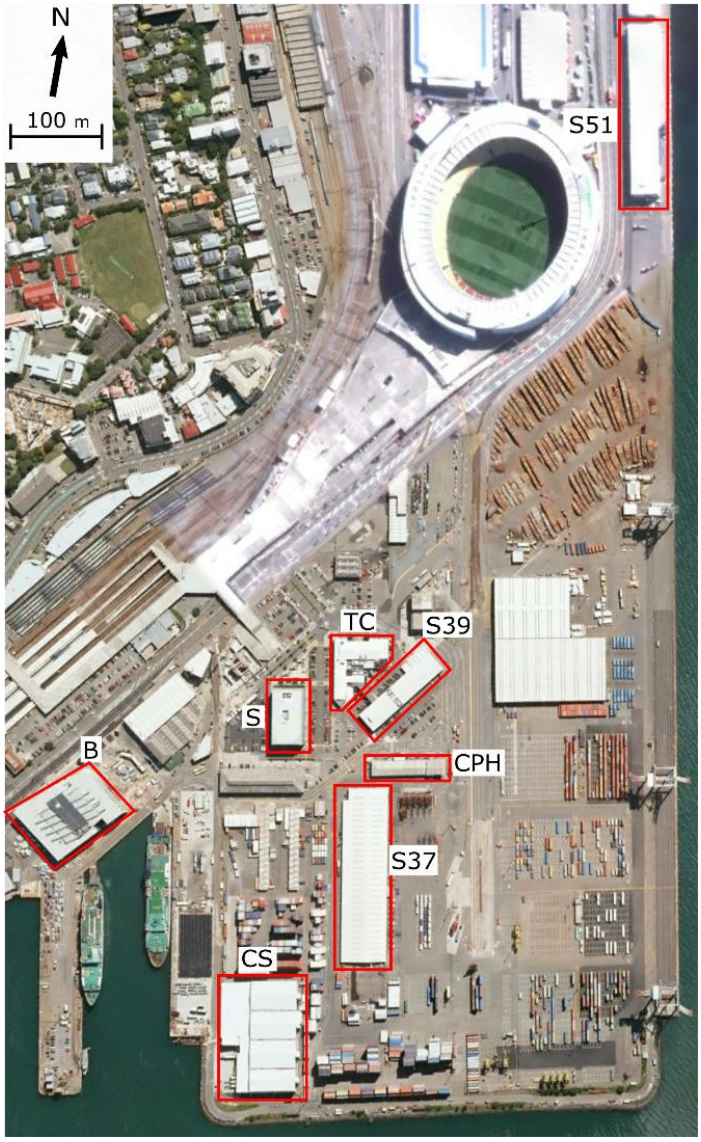

Figure 7.1: CentrePort Wellington map identifying buildings studied in this reconnaissance. (Base image from Google Earth™)

7.2 Buildings on Shallow Foundations

7.2.1 CPH Building

The CPH building (S41.27829° E174.78618°) is founded on reinforced concrete (RC) spread footings connected with RC grade beams (Figure 7.2). There were no apparent signs of structural distress, and the building was operational at the time of the reconnaissance in late November 2016. The building and surrounding fill settled relatively uniformly, however, ground a few meters to the west of the CPH building did not appear to settle significantly as it was elevated relative to the surrounding ground and the floor level of the CPH building. The elevated ground was likely supported by the old bulkhead piles of the demolished Pipitea Wharf (see Figure 2.2), which minimized liquefaction-induced settlement of the ground and pavement above it. The building and fill settled approximately 230 to 260 mm relative to the ground supported on piles, as shown in Figure 7.3. Settlement appeared to be more or less uniform across the building footprint, as there were no apparent signs of relative movement or tilt of the ground floor of the CPH building from the visual investigation. However, a preliminary analysis of the LiDAR scans indicate a slight tilt (i.e., of 0.105 degrees) in the large operations room on the east end of the building.

Figure 7.2: Uniform settlement of CPH building which is founded on shallow foundations that apparently displaced downward the same amount as the surrounding fill. This photo is looking northeast at the southwest corner of the building. (S41.278395° E174.785639°, taken at 1230 hrs on 21NOV16)

Figure 7.3: Uniform settlement (230-260 mm) of the building relative to ground supported on old bulkhead piles of Pipitea Wharf. Looking north along western wall of CPH building. The perimeter walkway slopes down towards the building at 11 degrees over 1.35 meters. (S41.278395° E174.785639°, taken at 1225 hrs on 22NOV16)

7.2.2 CS Building

The CS building (S41.28105° E174.78483°) is supported on a composite shallow foundation with RC spread footings and mats. The building consists of an irregular-shaped single-story open loading bay in its western part (herein called the Shed) and a rectangular-shaped large cold storage facility on its eastern part (herein called the Freezers). The structural frames and supporting foundations of these two parts of the building appear to be independent. From observation, the structural system of the Shed is composed of concentrically-braced steel frames. The QuakeCoRE-GEER team members were given access to the Shed (i.e., the western part of the building) but not to the Freezers (i.e., the eastern part of the building). We did have access to the ground surrounding the building.

The differential ground movements across the building footprint induced structural deformation in the CS building. Seaward lateral ground movements on the order of 1 m occurred towards the western and southern slopes in the southwest corner the CentrePort reclaimed land. Figure 7.4 shows the location of six transects along which the location and width of lateral ground cracks in the pavement surrounding the CS building were recorded. Superimposed on this figure are plots of cumulative lateral ground displacement as a function of distance from the crest of the waterfront slopes for each transect. They show that, at the south side of the building, the fill moved towards the sea (southward) approximately 0.8 to 1.3 m. Similarly, the fill moved 0.8 to 1.1 m to the west direction. The top plot in Figure 7.4 indicates that the foundations of the building were subjected to a lateral stretch of approximately 200 mm. This stretch occurred over a column span of approximately 8.8 m, which corresponds to a lateral strain of about 2.3 percent. Tables 7.1 and 7.2 provide the measured crack widths and distances from the transect reference point for the east-to-west

(CS-1, CS-2, and CS-6) and north-to-south (CS-3, CS-4, and CS-5) transects, respectively. Data for all six transects are plotted in Figure 7.5.

Significant separation between the CS building foundation and pavement slab were observed on the south side of the building (as well as settlement and spreading of the surrounding pavement). Figure 7.6 shows a LiDAR scan documenting this separation, which ranges from 30 mm (west) to 230 mm (east).

Gravelly liquefaction ejecta was observed around the building (Figure 7.7). Figure 7.8 shows lateral ground movements and partial collapse of the slope at the reclamation edge along the western wall of the Shed of the CS building (which is parallel and adjacent to King's Wharf), where the ground settled approximately 530 mm relative to the King's Wharf. This part of the building is closest to the crest of the slope and it underwent the largest lateral movement. Figure 7.9 shows lateral movements near the crest of the western slope, and Figures 7.10 and Figure 7.11 show lateral spreading towards the southern slope with a vertical offset of approximately 1.1 m. In these large cracks and vertical offsets, shallow soils beneath the pavement were visible and consist of gravelly quarry rock reclamation fill. Crack widths and locations along the bottom of the outside walls of the CS building were also measured. Figure 7.12 shows results of this survey, which are consistent with the previously described lateral spreading measurements and indicate a lateral stretch of the shallow foundation of the Shed of approximately 200 mm in the westward direction.

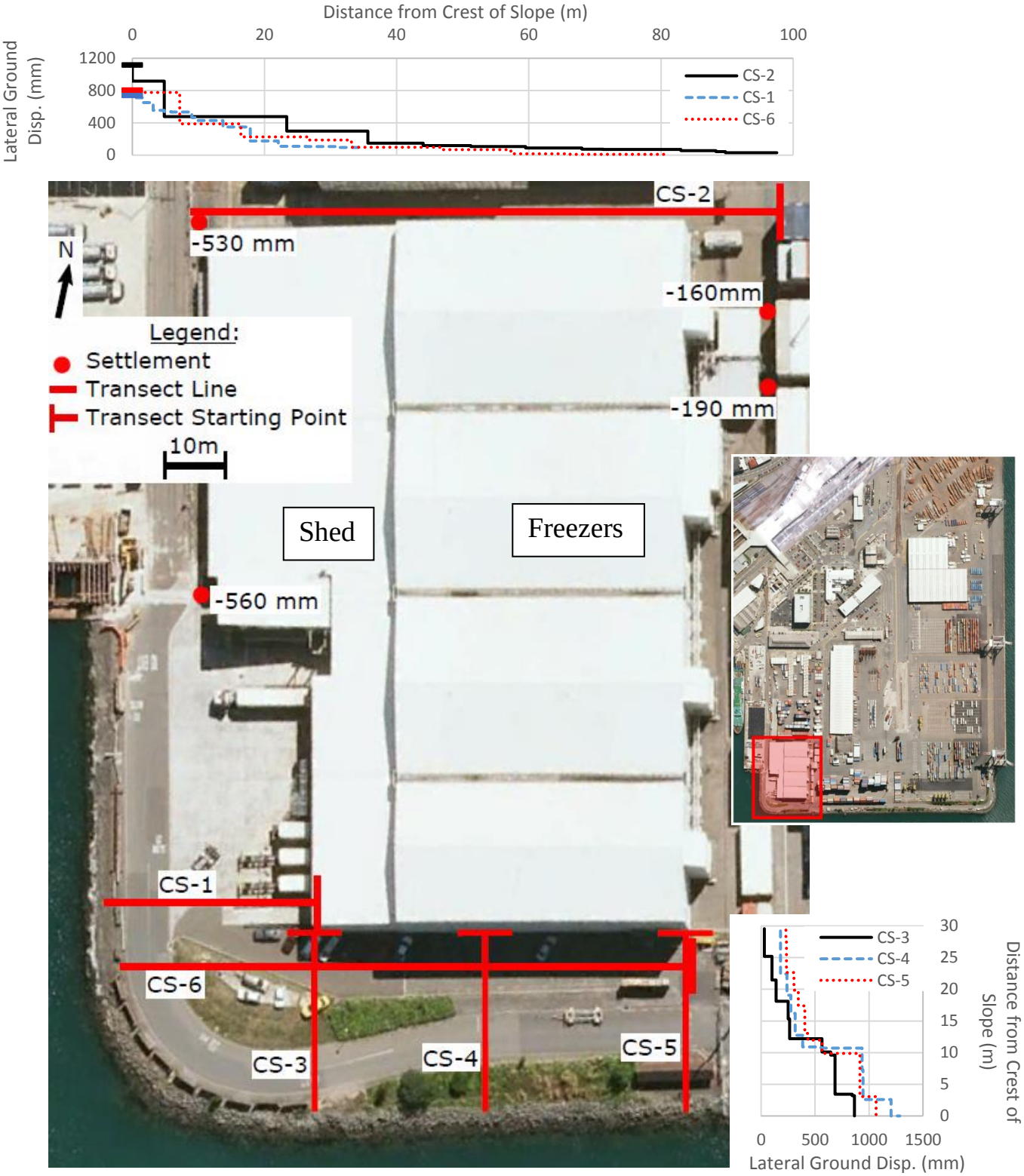

Figure 7.4: CS building lateral ground movement transects and vertical settlement measurement locations. Cumulative ground displacement versus distance from crest of slope are provided. Note that the crest of slope is further east at CS-2 than at CS-1 and CS-6, therefore, displacement plots do not perfectly align with satellite image for CS-2. Settlement measurements to the northeast are relative to the building which also settled.

Table 7.1: CS Building east-to-west lateral ground movement transects.

CS-1		CS-2		CS-6		
Horizontal Distance from Reference Point (m)	**Crack Width (mm)**	**Horizontal Distance from Reference Point (m)**	**Crack Width (mm)**	**Horizontal Distance from Reference Point (m)**	**Crack Width (mm)**	**Vertical Offset (mm)**
1.06	95	0.00	30	14.43	10	0
4.21	10	7.80	15	28.60	7	0
9.03	5	9.20	10	37.56	50	0
13.17	65	14.50	15	48.16	30	-5
17.40	175	26.30	5	61.69	90	0
21.55	80	29.50	12	68.11	40	-2
25.60	35	38.00	20	78.42	160	-30
26.26	70	46.30	10	87.68	390	-210
29.42	5	53.50	30	94.84	30	-5
30.42	15	61.90	150	–	–	–
32.10	95	74.17	180	–	–	–
33.75	60	92.70	440	–	–	–
35.25	30	97.53	200	–	–	–
Total:	740	Total:	1,117	Total:	807	-252

Table 7.2: CS Building north-to-south lateral ground movement transects.

CS-3			CS-4			CS-5		
Horizontal Distance from Reference Point (m)	**Crack Width (mm)**	**Vertical Offset (mm)**	**Horizontal Distance from Reference Point (m)**	**Crack Width (mm)**	**Vertical Offset (mm)**	**Horizontal Distance from Reference Point (m)**	**Crack Width (mm)**	**Vertical Offset (mm)**
0.05	30	0	0.00	180	-30	0.33	230	0
4.40	70	0	6.80	60	0	2.02	5	0
8.15	40	0	10.15	35	0	7.02	70	-45
11.50	110	-10	13.00	40	-30	9.80	40	0
14.30	15	0	16.50	70	-150	12.30	60	60
17.40	300	-250	18.30	170	-25	16.64	30	-65
19.50	80	90	18.52	380	-770	17.72	130	90
20.00	40	10	21.98	10	0	19.82	350	-470
26.20	160	50	26.64	260	0	26.62	150	0
26.43	20	0	29.22	80	-105	29.68	35	0
29.62	0	-360	–	–	–	–	–	–
Total:	865	-470	Total:	1,285	-1110	Total:	1,100	-430

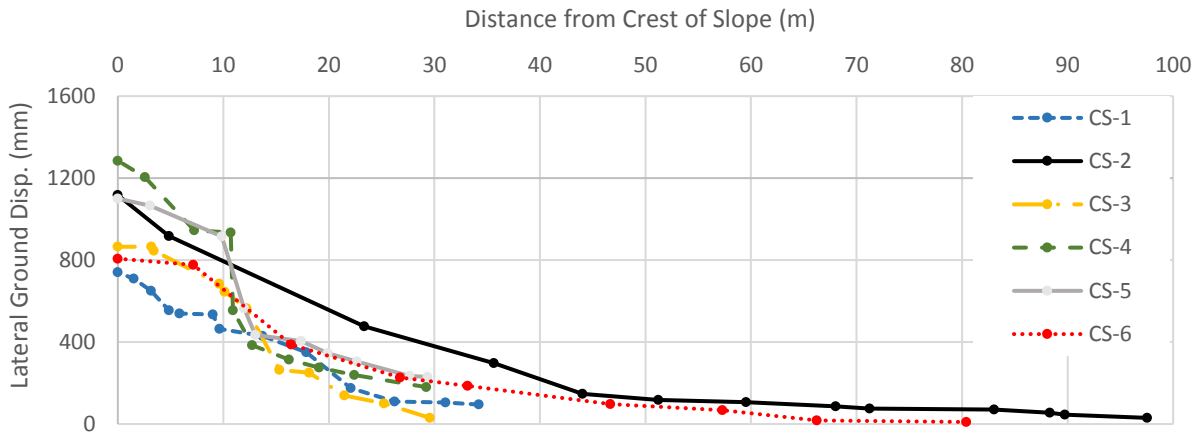

Figure 7.5: Cumulative lateral ground displacement versus distance from the crest of the waterfront slope for Cold Store lateral spread transects.

Figure 7.6: Perspective view of LiDAR scan looking westward showing the horizontal separation from building foundation and settlement of pavement observed on the south side of the CS building looking west (colored indicates intensity). The separation varies from 0.23 m wide to 0.03 m wide horizontally from the building's eastern side to its western side.

Figure 7.7: Gravelly liquefaction ejecta looking east along the northern wall of the CS building. (S41.280528° E174.784984°, taken at 1651 hrs on 22NOV16)

Figure 7.8: Looking north along the west wall of the CS building. The ground settled approximately 530 mm relative to the pile-supported bulkhead of King's Wharf, which is shown at the left side of the photograph. (S41.280923° E174.784389°, at 1411 hrs on 21NOV16)

Figure 7.9: Ground cracks in area west of the CS building and along the southwestern slopes of CentrePort (looking south). The CS building can be partially seen on the upper left corner of the photograph. (S41.281478° E174.784430°, taken at 1418 hrs on 21NOV16)

Figure 7.10: Approximately 1.1 m of vertical offset resulting from the southward lateral movement of the southern edge of CentrePort reclaimed land near its western side. Looking west near the southern wall of the CS building. (S41.281701° E174.785268°, taken at 1427 hrs on 21NOV16)

Figure 7.11: LiDAR scan of damage to the asphalt pavement and concrete curbs on the access road located south of the CS building. The vertical offset is approximately 1.1 m. This view is looking to the northeast.

Figure 7.13 documents significant cracking resulting in exposure of rebar in the foundation of the CS building on the north side from a LiDAR scan. Figure 7.13(a) looks south at the north wall of the CS building while Figure 7.13(b) shows the same crack running northward. The width of this crack is fairly consistent at 200 mm for much of the length as was observed in the LiDAR scan; however, it widens to 500 mm at some locations in the north and narrows to approximately 180 mm closer to the building (minimum width is 150 mm).

The western part of the CS building (i.e., the Shed) is a steel-frame, single-story structure with an open bay. As can be seen on the satellite image of the crack map shown in Figure 7.12, the total span of the Shed on its north end is about twice as wide as its span width on its south end. The northwest part of the Shed is closest to the free-face of the slope (Figure 7.8), and consequently experienced the largest lateral ground movement. Thus, the northern part of the Shed displacement laterally westward more than its southern end. The westward lateral movement of the north end of the building separated the Shed from the Freezers along the northern half of the building (Figure 7.14a). The differential lateral ground movements across the north-south length of the Shed produced deformations, cracks, and openings in the overlying foundation and structure. This deformation pattern was apparent by comparing the magnitude of building cracks along the north wall to those on the south wall, as well as separation of construction joints in the interior floating slab of the Shed. Measurements of construction joint separation in the slab are shown schematically in Figures 7.15 and 7.16 for the northern and southern parts of the Shed, respectively. Figure 7.17 was taken inside the Shed part of the CS building and shows construction joint separations. Figure 7.18 shows panoramic imagery co-acquired with the LiDAR data that can also be utilized for measurements. The maximum separation between slabs was measured to be 230 mm.

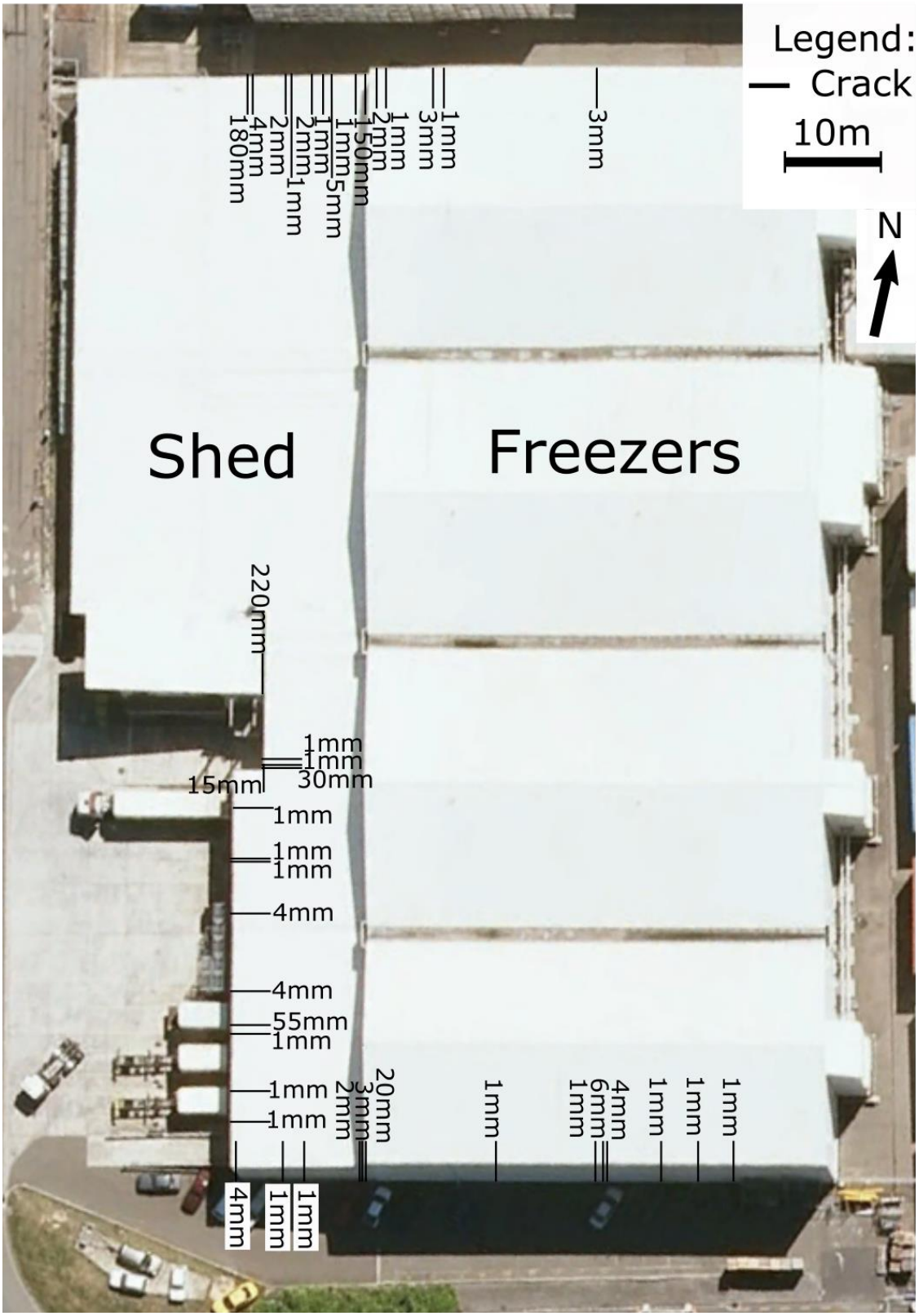

Figure 7.12: Location and width of lateral ground movement-induced cracks in the RC concrete walls at the base of the exterior building walls of the CS building. Crack openings are parallel to each wall.

(a)

(b)

Figure 7.13: (a) Significant damage and cracking observed in the LiDAR scan data at the north end of the CS building. (b) The same crack extending northward across the port.

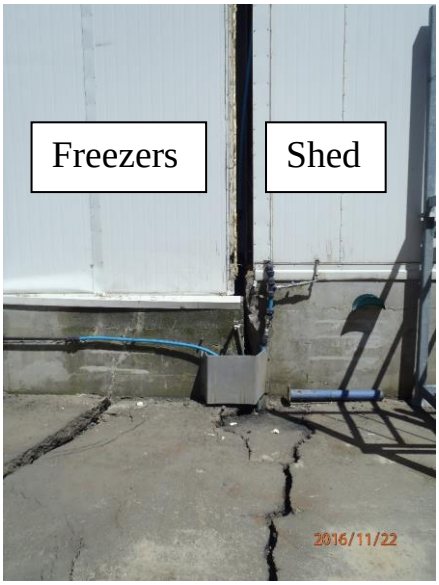

(a)

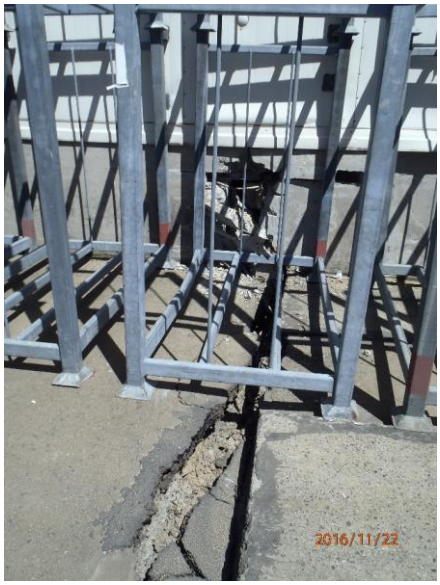

(b)

Figure 7.14: Cracks along the exterior north wall of CS building: (a) 150 mm of separation between Shed and Freezers (i.e., westward/seaward movement of the Shed relative to the Freezers), (S41.280584° E174.784705°, taken at 1445 hrs on 22NOV16), and (b) 180 mm crack in the shed from westward lateral spreading (also shown in Figure 7.13b). (S41.280607° E174.784533°, taken at 1444 hrs on 22NOV16)

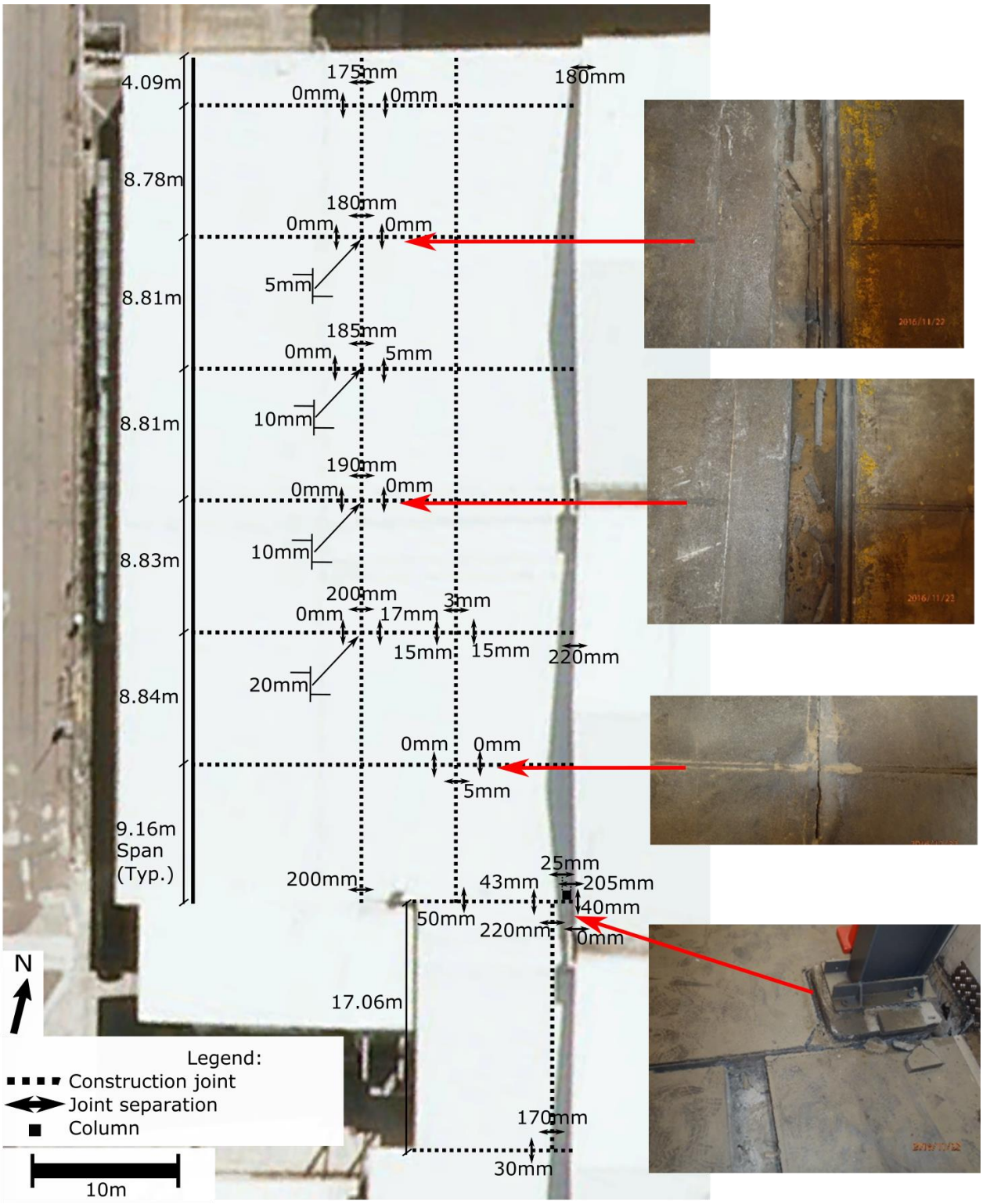

Figure 7.15: Northern part of Shed floor slab contraction joint separation measurements. Photographs along right side of figure are of contraction joints at which measurements were taken and are aligned vertically with each depicted joint. (Taken 22NOV16)

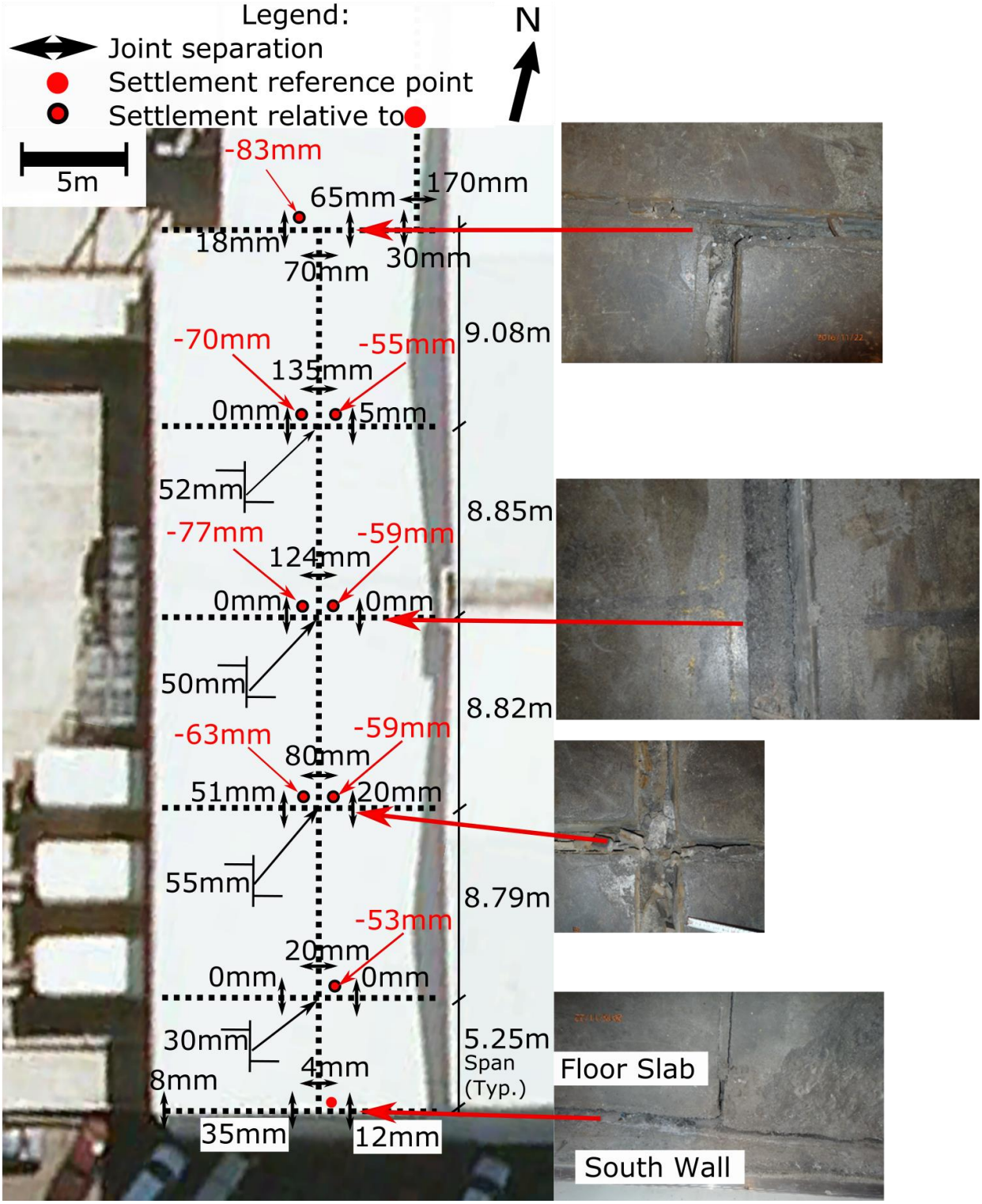

Figure 7.16: Southern part of Shed floor slab contraction joint separation measurements. Photographs along right side of figure are of contraction joints at which measurements were taken and are aligned vertically with each depicted joint. (Taken 22NOV16)

Figure 7.17: Contraction joint separation of ground floor slab inside the Shed of CS building looking south. As shown in photo, joint separations occurred in two orthogonal directions. (S41.281255° E174.784797°, taken at 1520 hrs on 22NOV16)

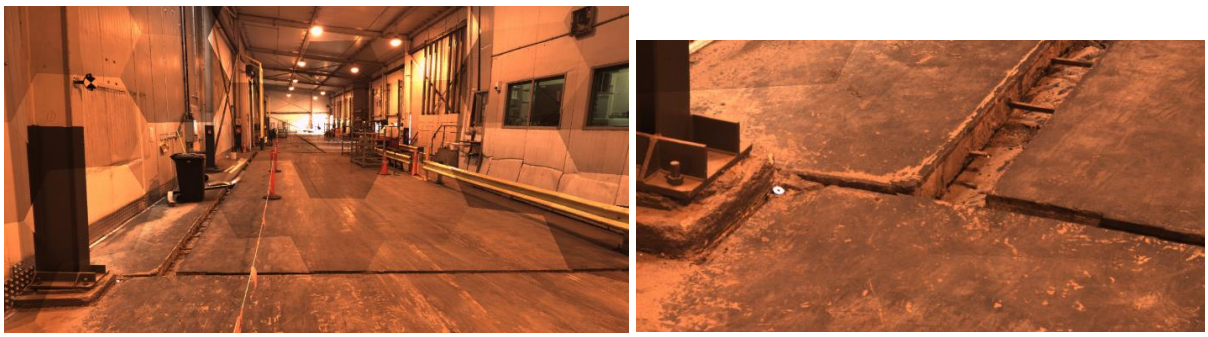

(a) (b)

Figure 7.18: Example panoramic imagery co-acquired with the laser scans: (a) overview, and (b) close-up of floor separation in the CS building. The larger crack measures 230 mm in width and the smaller crack measures 75 mm in width.

The differential lateral ground movements across the footprint of the Shed part of the CS building were also manifested in the deformation pattern of its steel framing. This deformation pattern is shown in Figures 7.19 and 7.20. Figure 7.19 is a photograph of the second frame from west to east along the north wall (i.e., the third, easternmost, bay is not shown in this sketch). Figure 7.20 is a schematic of the three west-most columns along the north wall looking north from the interior. The western-most column span along the north wall was measured as 8.663 m from column centerline to centerline at a height of 1.5 m above the floor slab. The next span to the east was measured as 8.789 m in the same way. In addition to the tilting of these columns along the north wall, at least two columns along the east wall of the shed were rotated at the base, causing buckling of the concentric bracing between columns (Figure 7.21).

Figure 7.19: Internal north wall of Shed of CS building showing 1.5° clockwise tilt of the left column (2nd column from the west along north wall), and 2° counterclockwise tilt of the right column (3rd column from the west along north wall). This deformation was caused by a 180 mm opening in the RC base wall, which is visible in the bottom middle of the photograph where light is entering building. This column span is 8.789 m from centerline of column to centerline at a height of 1.5 m above the floor slab. (S41.280626° W174.784450°, taken at 1452 hrs on 21NOV16)

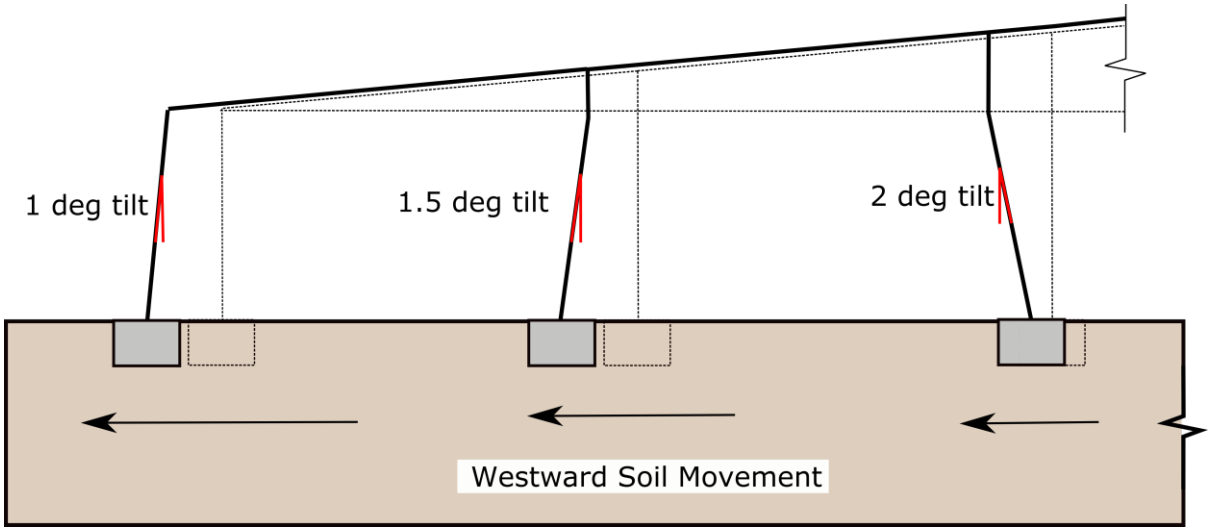

Figure 7.20: Schematic of deformation pattern of steel frame along the north wall of CS building (3 west-most columns of the Shed; looking north from interior).

Figure 7.21: Internal east wall in northern part of the Shed, which shows column-pedestal connection failure due to rotation of the base of the column and buckling of concentric bracing. (Approx. at S41.280939° E174.784778°, taken at 1615 hrs on 22NOV16)

7.3 Buildings on Deep Foundations

7.3.1 S39 Building

The S39 building is supported on Frankie piles. The old buried mass concrete seawall (i.e., Old Seawall) runs parallel and adjacent to the southeast wall of the building. Additionally, along the southeast wall, a segment of the historic Fryatt Quay Wharf deck (Figure 2.2) was left intact. The ground to the south of the seawall and wharf settled 220 mm relative to the top of the wharf deck and the pile-supported building (Figure 7.22). Approximately 100 to 190 mm of settlement was observed along the south west wall of the building (Figure 7.23). On the northwest side of the building, the ground adjacent the building settled approximately 50-100 mm relative to the building (Figure 7.24). The QuakeCoRE-GEER team was informed that the ground floor slab dropped 150 mm inside the building (T+T (2016), private communication).

Figure 7.22: Southeast side of Building S39 and a buried segment of the Fryatt Quay Wharf deck parallel to the building. Fill to the south of the buried mass concrete seawall/wharf settled 220 mm relative to the pile-supported building and wharf deck. (S41.277984°, E174.785776°, taken at 1230 hrs on 22NOV16)

Figure 7.23: Looking southeast along southwest wall of S39. Fill settled approximately 190 mm relative to pile-supported building at the northwest corner of the building (shown on lower left corner of photo), and magnitude of settlement decreased south-eastward along this wall. (S41.277994°, E174.785467°, taken on 17NOV16)

Figure 7.24: Looking southwest along northwest wall of S39. Fill settled 50-100 mm relative to pile-supported building. (S41.277882°, E174.785371°, taken on 17NOV16)

7.3.2 TC Building

The TC building is immediately to the northwest of the S39 building, and is supported on driven RC piles. Liquefaction ejecta was observed along the short southwest wall of the building, and 150 mm of ground settlement relative to the building was measured (Figure 7.25).

Figure 7.25: Southwest wall of TC building with liquefaction ejecta and 150 mm of ground settlement relative to building. (S41.277858°, E174.785081°, taken at 1246 hrs on 22NOV16)

7.3.3 S37 Building

The western half of the S37 building is founded on the deck of the buried, partially demolished pile-supported old Pipitea Wharf, and the east wall of the building is supported on piles. The precast seawall that formerly ran along the bulkhead of the Pipitea Wharf is now buried and runs south-to-north through about the centerline of the building. The ground floor slab not supported either on piles, the old wharf deck, or the precast seawall settled up to 550 mm relative to these structures (Figures 7.26 and 7.27; and 7.28 from LiDAR scan). The ground settled approximately 375 mm relative to the building along the exterior of the east wall of the S37 building (Figure 7.30). Figure 7.28 plots elevations from transect LT6 (see Figure 5.2 for transect location) through the S37 Building, and Figure 7.29 provides a 3D view of the building interior from a LiDAR scan. Approximately 16 m west of the western wall of the S37 building, a buried row of piles from the old Pipitea Wharf protruded from the ground as the surrounding fill settled approximately 300 mm relative to the piles (Figure 7.31).

Figure 7.26: Looking west across inside of the S37 building. Approximately 400-550 mm of differential settlement between the ground and the buried precast concrete seawall that runs south-to-north through the center of the building. (S41.279065°, E174.785787°, taken at 1220 hrs on 21NOV16)

Figure 7.27: Looking west across north wall of Building S37. Approximately 400mm of differential settlement between ground and deck of buried, pile-supported Pipitea Wharf that supports the western side of the shed. (S41.278571°, E174.785632°, taken at 1227 hrs on 21NOV16)

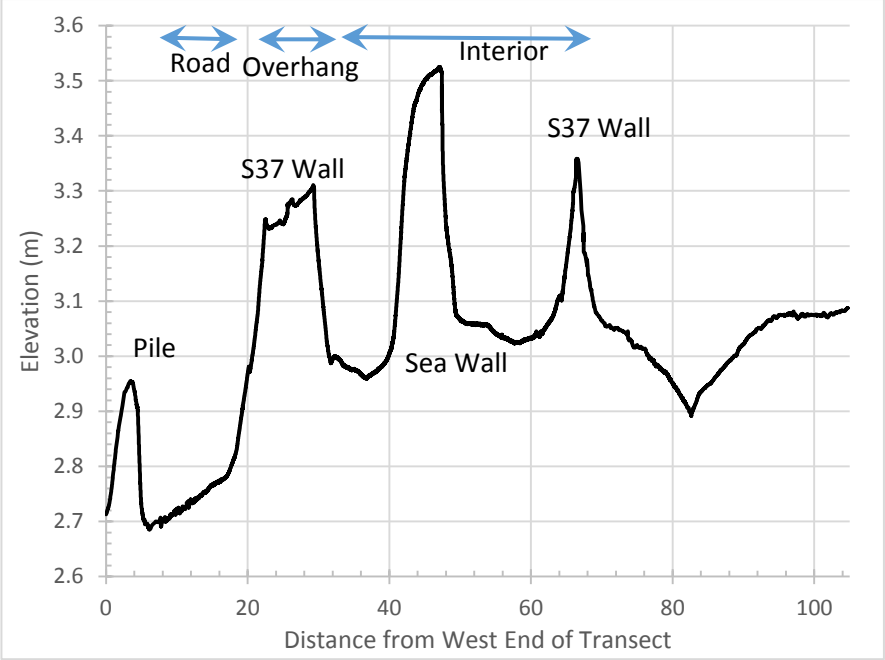

Figure 7.28: East-west cross-section (LT6) through the northern part of Building S37. Note the significant vertical exaggeration.

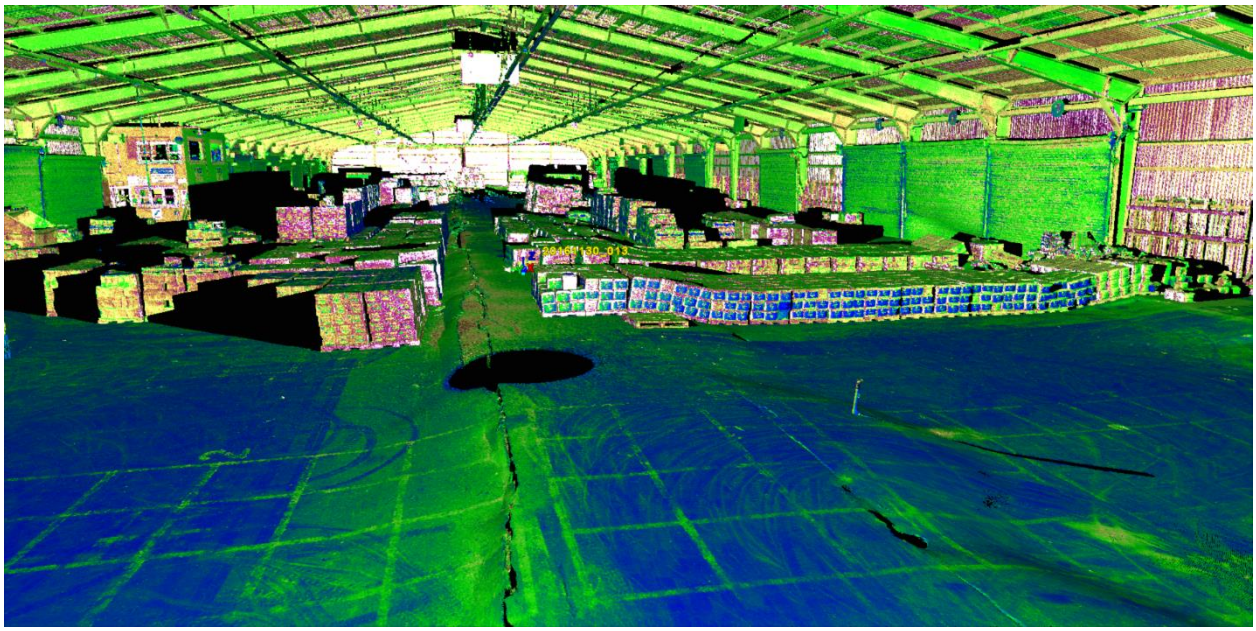

Figure 7.29: LiDAR scan obtained inside Building S37 showing cracking and settlement of the pavement around the buried precast concrete seawall (up to 550 mm of differential settlement occurred).

Figure 7.30: Looking south along east wall of Building S37, which shows approximately 375 mm of differential settlement between fill and pile-supported east wall of the building. (S41.279065°, E174.785787°, taken at 1220 hrs on 21NOV16)

Figure 7.31: Looking south along western-most row of piles from partially demolished and buried Pipitea Wharf, which is approximately 16 m west of Building S37. Fill settled 300 mm relative to embedded piles (S41.278798°, E174.785186°, taken on 17NOV16). A cross section (LT1) is shown in Figure 5.4.

7.3.4 S51 Building

The S51 building is in the northeastern reclaimed land of CentrePort Wellington. This area of the port was reclaimed using hydraulically-placed dredged fill. The eastern wall of the building is founded on the pile-supported wharf, and the remainder of the building is founded on piles. The ground south of the building settled 230 mm relative to the wharf deck (Figure 7.32). Settlement magnitudes decreased from south to north, and only 10 to 20 mm of ground settlement was observed relative to the wharf in the surrounding ground north of the building. The wharf that supports the eastern wall moved laterally eastward approximately 85mm (35 mm crack at bulkhead and 50 mm crack 14.6 m west of bulkhead), which resulted in cracking of the southern wall near the wharf bulkhead (Figure 7.32). This equates to 85 mm of lateral movement over 14.6 m corresponding to a lateral strain of approximately 0.58 percent. Additionally, several vertical cracks were observed in the western exterior walls of the building (Figure 7.33).

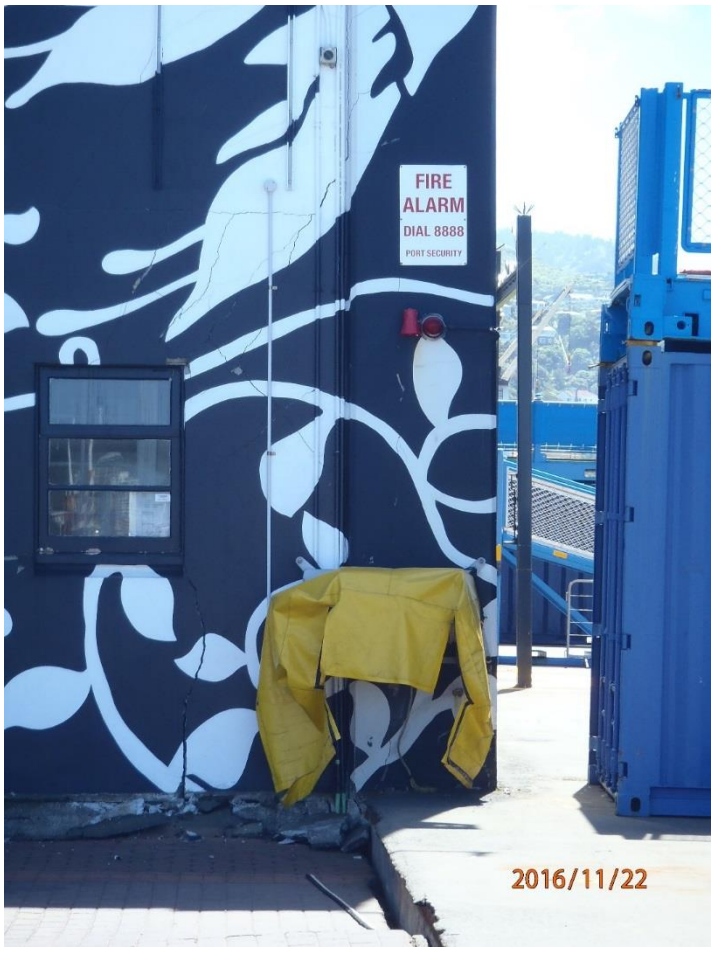

Figure 7.32: Southeast corner of Building S51 looking north, which shows 230 mm of differential settlement between wharf that supports its east wall and the inland fill. Also visible is 35 mm crack from seaward movement of wharf relative to adjacent ground. (S41.272404°, E174.787815°, taken at 1303 hrs on 22NOV16)

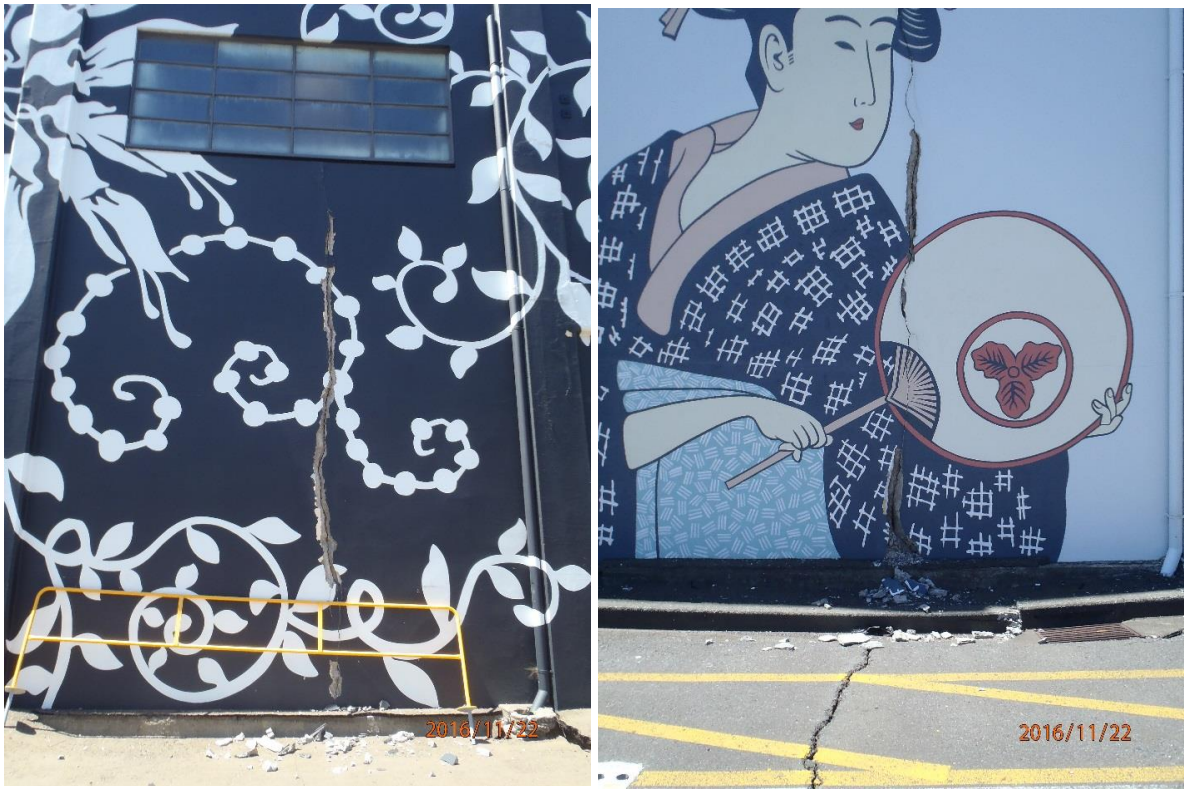

Figure 7.33: Vertical cracks along exterior west wall of S51 located at approximately 25 meters (left photo), and 60 meters (right photo) north of the southwest building corner. (Left: S41.272224°, E174.787391°, taken at 1316 hrs on 22NOV16. Right: S41.271906°, E174.787307°, taken at 1312 hrs on 22NOV16)

7.3.5 S Building

The S building is a relatively new (i.e., constructed in 2006) 5-storey reinforced concrete building founded on piles. The corners are on driven reinforced concrete piles while the interior columns are founded on cast-in-place concrete piles. No ground improvement was performed under the building. The building suffered structural damage, and is being investigated thoroughly by CentrePort. The interested reader is referred to publications that will be forthcoming by others. No signs of foundation damage were visible at the ground surface during the QuakeCoRE-GEER team visit though some level of distress in the ground adjacent to the building was evident. The ground settled 100 to 200 mm relative to the pile-supported building (Figure 7.34), in a relatively uniform fashion though some deviations from this pattern were also evident. Ground floor infill walls along the perimeter of the building were cracked in places (Figure 7.35), and the Level 1 floor slab pulled out and partially collapsed (Figure 7.36).

Figure 7.34: Looking west at southeast corner of the S building at which fill settled approximately 100 to 200 mm relative to pile-supported building. (S41.278285°, E174.784757°, taken at 1243 hrs on 21NOV16)

Figure 7.35: Damage to ground floor infill wall on the east side of the S building (S41.278114°, E174.784715°, 1241 hrs on 21NOV16)

Figure 7.36: Pull-out and partial collapse of Level 1 floor slab in the S building taken along the west wall of the building. (S41.277982°, E174.784255°, taken at 1246 hrs on 21NOV16)

7.3.6 B Building

The B building is supported on piles with stone column ground improvement performed over the southeastern (seaward) half of the building footprint. The surrounding ground settled approximately 50 to 90 mm uniformly relative to the building (Figure 7.37). No other significant movements were observed.

(a) (b)

Figure 7.37: Ground settlement relative to the pile-supported B building at: (a) the southwest corner of the building with ground improvement (S41.279767°, E174.782100°), and (b) northwest corner of the building without ground improvement (S41.279419°, E174.781443°). (taken at 1350 hrs on 21NOV16)

8. REFERENCES

Anderson, G. (1984). *Fresh about the Cook Strait – An appreciation of Wellington Harbour*. Methuen Publications, p.215.

Boulanger, R.W. and Idriss, I.M. (2012). Probabilistic Standard Penetration Test-Based Liquefaction-Triggering Procedure. *J. of Geotech. Geoenviron. Eng*., 138, 1185-1195

Boulanger, R.W. and Idriss, I.M. (2014). CPT and SPT Based Liquefaction Triggering Procedures. *Report No. UCD/CGM-14/01*, Center for Geotechical Modeling, Department of Civil and Environmental Engineering, University of California, Davis, April 2014.

Bradley, B. A., H. N. T. Razafindrakoto and V. Polak (2017). Ground motion observations from the 14 November 2016 Mw7.8 Kaikoura, New Zealand earthquake and insights from broadband simulations, *Seismological Research Letters*, 88(3): 740-756.

Greater Wellington Regional Council: http://graphs.gw.govt.nz/?siteName=Wellington%20at%20Te%20Papa&dataSource=Rainfall&interval=1%20Hour&Alignment=1%20Hour (Accessed 11 May 2017)

Hutchison, A. J. H. (1973). Reclamations in Wellington Harbour with special reference to recent developments. *New Zealand Engineering*. 15 August 1973, 217-224.

Idriss, I.M. and Boulanger, R.W. (2008) Soil Liquefaction during Earthquakes. Earthquake Engineering Research Institute, Monograph-12, Oakland, California, USA.

Kayen R., Stewart, J.P. and Collins B. (2010). Recent advances in terrestrial LIDAR applications in geotechnical earthquake engineering. In *5th International Conference on Recent Advances in Geotechnical Earthquake Engineering and Soil Dynamics*, 24– 29 May 2010, San Diego, CA (Rolla, MO: Missouri University of Science and Technology), p. 8.

Olsen, M.J. and Kayen, R. (2012). Post-earthquake and tsunami 3D laser scanning forensic investigations, *ASCE Forensics Conference 2012*, San Francisco, California. CD-ROM.

Olsen, M.J., Wartman, J., McAlister, M., Mahmoudabadhi, H., O'Banion, M.S., Dunham, L. and Cunningham, K. (2015). To fill or not to fill: Sensitivity analysis of the influence of resolution and hole filling on point cloud surface modeling and individual rockfall event detection, Remote Sensing, Special Issue - *Use of LiDAR and 3D point clouds in geohazards*, 79(9),12103-12134. doi:10.3390/rs70912103

Semmens, S., Dellow, G. D., and Perrin, N.D. (2010). It's Our Fault – Geological and Geotechnical Characterisation of the Wellington Central Business District. *GNS Science Consultancy Report* 2010/176. 52p.

SNZ (2004). "NZS 1170.5: Structural Design Actions – Part 5 Earthquake Actions – New Zealand". *Standards New Zealand*, Wellington, NZ.

Tonkin & Taylor Ltd. (1998). Proposed Coldstore Geotechnical Report. Prepared for CentrePort Limited. Ref No. 82363.

Tonkin & Taylor Ltd. (2000). CentrePort Shed R Geotechnical Report. Prepared for CentrePort Limited. Ref No. 82787-01.

Tonkin & Taylor Ltd. (2006). Harbour Quays Development Factual Geotechnical Report, Revision 2. Prepared for CentrePort Wellington Limited. Ref No. 83725.004

Tonkin & Taylor Ltd. (2012). Thorndon Container Wharf Seismic Assessment Geotechnical Factual Report. Prepared for CentrePort Limited. Ref No. 85369.001.

Tonkin & Taylor Ltd. (2014). Thorndon Container Wharf Seismic Assessment Geotechnical Interpretive Report. Prepared for CentrePort Limited. Ref No. 85369.001.